University of Bath

Aqueous Ozonation of Furans: Kinetics and Transformation Mechanisms Leading to the Formation of α,β-Unsaturated Dicarbonyl Compounds

Garyfalia A. Zoumpouli[a,b,c,d,1], Zhuoyue Zhang[d], Jannis Wenk[b,c], and Carsten Prasse[d,e,*]

[a] Centre for Doctoral Training, Centre for Sustainable Chemical Technologies, University of Bath, Bath BA2 7AY, UK.

[b] Department of Chemical Engineering, University of Bath, Bath BA2 7AY, UK.

[c] Water Innovation and Research Centre (WIRC), University of Bath, Bath BA2 7AY, UK.

[d] Department of Environmental Health and Engineering, Johns Hopkins University, Baltimore, MD 21218, USA.

[e] Risk Sciences and Public Policy Institute, Johns Hopkins Bloomberg School of Public Health, Baltimore, MD, United States

[1] Present address: Cranfield Water Science Institute, Cranfield University, College Road, Cranfield MK43 0AL, UK

Corresponding author

* To whom correspondence should be addressed:

Email: cprasse1@jhu.edu

Address: 3400 N Charles Street, Baltimore, MD 21218

Abstract

Despite the widespread occurrence of furan moieties in synthetic and natural compounds, their fate in aqueous ozonation has not been investigated in detail. Reaction rate constants of seven commonly used furans with ozone were measured and ranged from $k_{O3} = 8.5 \times 10^4$ to 3.2×10^6 M^{-1} s^{-1}, depending on the type and position of furan ring substituents. Transformation product analysis of the reaction of furans with ozone focusing on the formation of toxic organic electrophiles using a novel amino acid reactivity assay revealed the formation of α,β-unsaturated dicarbonyl compounds, 2-butene-1,4-dial (BDA) and its substituted analogues (BDA-Rs). Their formation can be attributed to ozone attack at the reactive α-C position leading to furan ring opening. The molar yields of α,β-unsaturated dicarbonyl compounds varied with the applied ozone concentration reaching maximum values of 7% for 2-furoic acid. The identified α,β-unsaturated dicarbonyls are well-known toxicophores that are also formed by enzymatic oxidation of furans in the human body. In addition to providing data on kinetics, transformation product analysis and proposed reaction mechanisms for the ozonation of furans, this study raises concern about the presence of α,β-unsaturated dicarbonyl compounds in water treatment and the resulting effects on human and environmental health.

Keywords: organic micropollutants, transformation products, reactivity-directed analysis, dicarbonyls, toxic by-products

Highlights

- Ozonation kinetics and transformation products of substituted furans were investigated
- High ozone reactivity of furans depending on type and position of substituents
- Identification of toxic α,β-unsaturated dicarbonyls using an amino acid reactivity assay
- Yields of toxic dicarbonyls are compound dependent and reached up to 7%

1. Introduction

Furans are heterocyclic aromatics comprising a five-membered ring of four carbons and one oxygen atom. The use of furan derivatives for the production of biomass-derived fuels, polymers and other chemicals has dramatically increased over the last decades (Eldeeb and Akih-Kumgeh, 2018; Gandini et al., 2016; Keay and Dibble, 1996; Tong et al., 2010). Furfural, a commodity chemical and precursor of many other furans, has a global production capacity of 280 kTon per year, with 65% used to produce furfuryl alcohol (Mariscal et al., 2016). In addition to their industrial applications, furans are common moieties in a variety of naturally occurring compounds including terpenes and fatty acids, and can be formed abiotically from the oxidation of natural organic matter (Hannemann et al., 1989; Huber et al., 2010; Wang et al., 2014). The extensive use of furan-containing chemicals and their natural occurrence make them likely contaminants in wastewater and drinking water resources as evidenced by the detection of furan-containing compounds, particularly pharmaceuticals, in wastewater effluent and surface water (Jelic et al., 2011; Kasprzyk-Hordern et al., 2008; Kostich et al., 2014).

Ozonation is increasingly used for the removal of trace organic contaminants in wastewater treatment, wastewater reuse and drinking water production (Gottschalk et al., 2009). Ozone is a selective oxidant that primarily reacts with electron-rich moieties such as double bonds (von Gunten, 2003; von Sonntag and von Gunten, 2012). Transformation products of the ozonation of organic compounds include carbonyls formed by cleavage of olefinic bonds or benzene rings, N-oxides and hydroxylamines by oxidation of amines, and sulfoxides by oxidation of thioethers (Hübner et al., 2015; Lee and von Gunten, 2016). The identification of ozone transformation products with (eco)toxicological implications is of importance (von Gunten, 2018). For example, the main ozonation product of carboxy-acyclovir inhibits the growth of green algae, an effect not observed for the parent compound (Schlüter-Vorberg et al., 2015). Similarly, embryotoxicity in a zebrafish assay was observed for the ozonation products of carbamazepine while no effects were observed for carbamazepine itself (Pohl et al., 2020).

Despite extensive research on the reaction of ozone with several classes of organic compounds including olefins, phenols and nitrogen-containing compounds (Zoumpouli et al., 2020), studies focussing on the transformation of furans during aqueous ozonation are limited. The dimethylfuran moiety present in the antacid drug ranitidine has been shown to contribute to the high reactivity of this compound with ozone (Jeon et al., 2016). However, no transformation products that are specific for the reaction of ozone with the furan moiety were

reported (Christophoridis et al., 2016; Zou et al., 2018). For the diuretic drug furosemide, two ozonation products were identified indicating the potential relevance of cleavage and/or opening of the furan ring by ozone (Aalizadeh et al., 2019).

Studies investigating the reaction of furans with ozone in organic solvents or organic solvent/water mixtures suggest the potential involvement of different reaction mechanisms (Bailey and Colomb, 1957; Bailey et al., 1965; Jibben and Wibaut, 1960; White et al., 1965). Jibben and Wibaut (1960) identified glyoxal (a C_2 dicarbonyl) as the sole ozone transformation product of furan and attributed its formation to the reaction of ozone with the two carbon-carbon double bonds (α-β bonds) of the furan ring, leading to a C_2 dicarbonyl containing both β-C atoms, and/or to β,β-addition of ozone, leading to two C_2 dicarbonyls that contain one α- and one β-C atom of the furan ring (see Table 1 for nomenclature). In contrast, Bailey and Colomb (1957) and Bailey et al. (1965) observed the formation of α,β-unsaturated dicarbonyl compounds containing all four carbons of the furan ring in experiments with diarylfurans such as 2,5-diphenylfuran. The results of Bailey et al. indicate the relevance of two distinct reaction pathways: (i) ozonolysis of a carbon-carbon double bond (α-β bond), and (ii) electrophilic ozone attack at the reactive α-C position in either a bidentate or monodentate manner, followed by ring cleavage to form a C_4 dicarbonyl (Bailey, 1982). These C_4 dicarbonyls then form lower-molecular weight transformation products through further reaction with ozone (Bailey, 1982).

Given the absence of kinetic and mechanistic information on the ozonation of furans in aqueous solutions, the aim of this study was to determine the ozonation kinetics of various commonly used furans and elucidate the formation of ozonation products in water. The specific focus was on the formation of toxic α,β-unsaturated dicarbonyl transformation products which have been recently identified as novel, highly-toxic by-products formed during the oxidation of phenols with various oxidants including hydroxyl radicals and chlorine (Prasse et al., 2018; Prasse et al., 2020). In addition, α,β-unsaturated dicarbonyls are also formed during the enzymatic oxidation of furans in the human body (catalyzed by cytochrome P450) and are responsible for their toxicity (Chen et al., 1995; Peterson, 2013; Ravindranath et al., 1984). The studied furans included two high usage pharmaceuticals (furosemide, ranitidine) that can be frequently found in the effluent of wastewater treatment plants (Kostich et al., 2014), and seven high production volume industrial chemicals (furfuryl alcohol, 2-furoic acid, 2,5-dimethylfuran, 2-methyl-3-furoic acid, 3-(2-furyl)propanoic acid, 3,4-bis(hydroxymethyl)furan, furan-2,5-dicarboxylic acid) (Eldeeb and Akih-Kumgeh, 2018;

123 Gandini et al., 2016). Transformation product formation was followed using liquid
124 chromatography-high resolution mass spectrometry (LC-HRMS). In addition, an amino acid
125 reactivity assay was used to specifically assess the formation of α,β-unsaturated dicarbonyls
126 that cannot be directly analysed with LC-HRMS due to the absence of ionizable groups in
127 these molecules (Prasse et al., 2018; Prasse et al., 2020).

128

129 **2. Materials and Methods**

130 *2.1 Chemicals*

131 Furfuryl alcohol (FFA, CAS no.: 98-00-0), 3,4-bis(hydroxymethyl)furan (BHF, CAS no.:
132 14496-24-3), 2,5-dihydro-2,5-dimethoxyfuran (CAS no.: 332-77-4), 2,5-dimethylfuran
133 (DMF, CAS no.: 625-86-5) in liquid form and 2-furoic acid (FA, CAS no.: 98-00-0), 2-methyl-
134 3-furoic acid (MFA, CAS no.: 98-00-0), 3-(2-furyl)propanoic acid (FPA, CAS no.: 935-13-
135 7), furan-2,5-dicarboxylic acid (FDCA, CAS no.: 3238-40-2), furosemide (FRS, CAS no.: 54-
136 31-9), ranitidine (RAN, CAS no.: 66357-59-3) in powder form were purchased from Sigma-
137 Aldrich or Fisher Scientific in high purity (≥97%). *N*-α-acetyl-lysine (NAL) was from Sigma
138 Aldrich (>98% purity). *N*-α-acetyl-cysteine (NAC) was from Fisher Scientific (>98% purity).
139 Solvents for analysis, salts for preparation of buffers and *tert*-butanol were from Fisher
140 Scientific. All experimental and analytical solutions, including stock solutions, were prepared
141 in ultrapure water (resistivity > 18 MΩ cm^{-1}) produced with a Milli-Q (Merck) or ELGA
142 (Veolia) water purification system.

143

144 *2.2 Ozonation experiments*

145 Competition kinetics experiments were performed to determine the second order rate
146 constants for the reaction of furans with ozone in pure water buffered at pH 7 (10 mM
147 phosphate buffer, 10 mM *tert*-butanol). RAN was used as the reference compound, due to its
148 known reaction rate constant with ozone (Jeon et al., 2016) and since initial tests had shown
149 that most of the target furans had an ozone reactivity within approximately one order of
150 magnitude of RAN. For compounds that reacted with ozone with much lower reaction rate
151 constants than RAN, FA was used as the reference compound, after determining its rate
152 constant using RAN. Further details on competition kinetics experiments and calculations are
153 provided in the SI, Supplementary text S1.

154 Batch ozonation experiments to study the formation of transformation products of furans were
155 performed in 20-mL amber glass vials. The reaction solutions (10 mL) contained 15 μM of

156 the target compound and 10 mM phosphate buffer (pH 7), diluted with ultrapure water. After
157 sampling the initial solution, a volume of concentrated ozone stock solution (see SI,
158 Supplementary text S1) was added to achieve concentrations of 4 to 65 μM ozone (0.3 to 4.3
159 μM O_3/μM target compound). The samples were left uncapped at room temperature for
160 approximately 2 hours to achieve residual ozone depletion. To assess the influence of OH
161 radical scavenging, a subset of experiments (Figures S2 and S3 in the SI) was also performed
162 with addition of 10 mM *tert*-butanol ($k_{OH, tert\text{-}butanol} = 6 \times 10^8 \text{ M}^{-1} \text{ s}^{-1}$) (Buxton et al., 1988).

163 Detection of α,β-unsaturated dicarbonyl compounds was accomplished using an amino acid
164 reactivity assay, which is described in detail elsewhere (Prasse, 2021; Prasse et al., 2018;
165 Prasse et al., 2020). The reaction of NAL with α,β-unsaturated dicarbonyls leads to the
166 formation of NAL adducts which can be detected using LC-HRMS (see section 2.3) (Prasse
167 et al., 2018). To this end, a small volume of a NAL stock solution was added to the samples
168 (final concentration 150 μM, equivalent to 10 times the initial concentration of the parent
169 compound) followed by incubation at room temperature for 24 hours. Selected experiments
170 were repeated with higher concentration of the target compound (up to 100 μM) to facilitate
171 the identification of α,β-unsaturated dicarbonyl transformation products. Additionally, for
172 some samples an equimolar mixture of NAL and NAC stock solutions was used instead of the
173 NAL stock solution, to enable the detection of dicarbonyls that do not form adducts with NAL
174 alone but do form NAC or NAL+NAC adducts (Prasse et al., 2018). All samples were
175 analyzed within 48 hours.

176

177 *2.3 Analytical approaches*

178 Spectrophotometric measurements to determine ozone concentrations were conducted in 1 cm
179 quartz glass cuvettes (Hellma) using a Cary 100 UV-VIS spectrophotometer (Agilent
180 Technologies), or in glass tubes using a DR/2000 Spectrophotometer (Hach).

181 Analysis of furans was performed using high-performance liquid chromatography with UV
182 detection (HPLC-UV). An overview of isocratic elution conditions, retention times and
183 detection wavelengths is provided in Table S1 of the SI. For batch ozonation a Vanquish
184 HPLC system with a DAD detector (Thermo Scientific) and an Acclaim RSLC 120 C18
185 column (5 μm, 120 Å, 4.6 × 100 mm) was used. For competition kinetics a Dionex UltiMate
186 3000 system with a DAD detector (Thermo Scientific) and an Acclaim RSLC 120 C18 column
187 (3 μm, 120 Å, 3 × 75 mm) was used.

188 The formation of ozonation products and NAL, NAC or NAL+NAC adducts was determined

189 via LC-HRMS using an UltiMate 3000 UHPLC system coupled to a Q Exactive HF Orbitrap

190 MS (both Thermo Scientific). For chromatographic separation, a Phenomenex Synergi Hydro-

191 RP column (4 μm, 80 Å, 1 × 150 mm) was used. External mass calibration was performed

192 every 5 days using a calibration mixture similar to procedures described previously (Prasse et

193 al., 2011). More information on LC-HRMS analysis is provided in the SI, Supplementary text

194 S2.

195 2-butene-1,4-dial (BDA), the α,β-unsaturated dicarbonyl identified in this work, was

196 quantified with standard addition calibration curves based on LC-HRMS analysis of its NAL

197 adduct, similar to a method described previously (Prasse et al., 2018). Stock solutions of BDA

198 (1 mM) were prepared through hydrolysis of 2,5-dihydro-2,5-dimethoxyfuran in ultrapure

199 water at room temperature for at least 24 hours. For each experiment, standard addition was

200 applied on one of the samples and the slope of the curve was used for the other samples of that

201 experiment. The limit of detection of BDA in ultrapure water buffered at pH 7 was 1 nM

202 (lowest standard with a signal-to-noise ratio >3) and the limit of quantification was 10 nM

203 (lowest standard with signal-to-noise ratio >10). Ozonation yields of BDA were calculated by

204 dividing the molar concentration of BDA with the molar concentration of the parent

205 compound that reacted (difference between initial and final concentrations). Yields of other

206 BDA analogues (BDA-Rs) without a standard available were estimated using BDA as
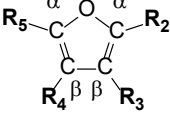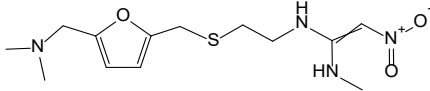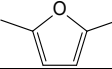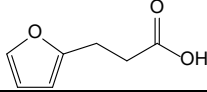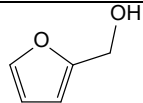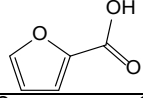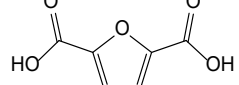
207 reference standard.

208
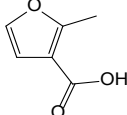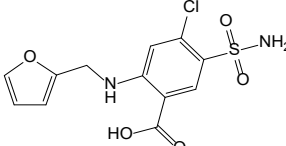
209 **3. Results and discussion**

210 *3.1 Kinetics of the reaction of substituted furans with ozone*

211 Table 1 shows the second order rate constants for the reaction of nine furans with ozone (k_{O3})

212 in water at pH 7, including two values that were available in the literature. The competition

213 kinetics plots for seven of the furans are provided in Figure S1. Initial tests indicated that the

214 studied furans have a high ozone reactivity, which was expected based on the aromaticity of

215 the furan ring. Competition kinetics experiments showed that the k_{O3} of FPA, MFA, FRS, FFA

216 and BHF varies only by a factor of 2 (1.7 (± 0.2) to 3.2 (± 0.2) × 10^6 M^{-1} s^{-1}), while reaction

217 rates for FA and FDCA were lower (5.9 (± 0.5) × 10^5 and 8.5 (± 0.7) × 10^4 M^{-1} s^{-1},

218 respectively). The ozone reactivity of most tested furans is comparable to that of phenols and

219 anilines at pH 7 (Lee and von Gunten, 2012).

220

Table 1. Second order rate constants for the reactions of furans with ozone in buffered water at pH 7. The ± error of each rate constant was calculated through error propagation from the 95% confidence interval of the slope of the linear fit and the error of the rate constant of the reference compound.

Compound	Structure	k_{O3} (M^{-1} s^{-1}) at pH 7	Reference
Substituted furan			
Ranitidine (RAN)		2.1×10^6	Jeon et al. (2016)
2,5-Dimethylfuran (DMF)		2.2×10^5	Jeon et al. (2016)
3-(2-Furyl)propanoic acid (FPA)		$(3.2 \pm 0.2) \times 10^6$	this study
2-Methyl-3-furoic acid (MFA)		$(2.7 \pm 0.1) \times 10^6$	this study
Furosemide (FRS)		$(2.2 \pm 0.1) \times 10^6$	this study
Furfuryl alcohol (FFA)		$(1.7 \pm 0.2) \times 10^6$	this study
3,4-Bis(hydroxymethyl)furan (BHF)		$(1.7 \pm 0.1) \times 10^6$	this study
2-Furoic acid (FA)		$(5.9 \pm 0.5) \times 10^5$	this study
Furan-2,5-dicarboxylic acid (FDCA)		$(8.5 \pm 0.7) \times 10^4$	this study

Our results suggest that steric effects due to the presence of substituents do not play an important role. A potential explanation for the unsignificant steric hindrance effect has been proposed by Bailey et al. (1965) for the ozonation of diarylfurans. Therefore, the observed differences of reaction kinetics are most likely attributable to the type of substituents (e.g. electron-withdrawing versus electron-donating) and their positions (e.g. located at an α-carbon versus at a β-carbon) on the furan ring. Electron-donating substituents such as hydroxyl and methyl groups increase the electron density of the furan ring and are therefore expected to

233 enhance its ozone reactivity, while electron-withdrawing groups such as carboxyl groups have
234 the opposite impact, similar to effects observed for phenols (Lee and von Gunten, 2012). The
235 three acids FPA, MFA and FA have pK_a values ranging from 3 to 4.4 (Arena et al., 1993),
236 hence they are all dissociated at pH 7. The carboxylate group exerts an electro-donating effect
237 in contrast with the carboxyl (Hansch et al., 1991), as is also evidenced by the similar ozone
238 reactivity of FA and FFA, which has an electron-donating hydroxymethyl substituent. MFA
239 had a higher rate constant than FA, due to the presence of an additional alkyl group and/or the
240 presence of a carboxylate substituent at a β- rather than an α-carbon. In FPA the carboxylate
241 group is separated from the furan ring by two additional carbons (C_2H_4 group) compared to
242 FA, leading to a 5-fold increase of the rate constant. Comparison of the kinetics of FDCA and
243 FA indicates that the presence of an additional carboxylate group (2,5-substitution of FDCA
244 versus 2-substitution of FA) lowers the ozone reactivity by approximately one order of
245 magnitude. The relatively low rate constant of DMF with ozone that has been reported in the
246 literature (Table 1) further indicates slower reaction kinetics for furans containing substituents
247 at both α-carbons (2,5-substitution). In contrast, BHF (3,4-substitution) had the same rate
248 constant as FFA (2-substitution), indicating that substituents located at β-carbons have a lower
249 impact on the reaction rates. Further experiments with a more diverse group of furan
250 compounds are necessary to develop Quantitative Structure-Activity Relationships (QSARs)
251 for substituted furans in oxidative water treatment processes similar to those that have been
252 developed for other compound classes such as phenols and amines (Lee et al., 2015; Lee and
253 von Gunten, 2012).

254 RAN contains multiple sites contributing to its high ozone reactivity: the furan ring, a tertiary
255 amine, a thioether and an acetamidine, which is the most reactive moiety (Jeon et al., 2016).
256 Similarly, the high rate constant of FRS can be attributed to both a furan ring and an aniline
257 moiety. Based on QSAR calculations, the k_{O3} of FRS has been reported as 6.8×10^4 M^{-1} s^{-1}
258 which was the sum of the contributions of the secondary amine ($pK_a = 3.8$, $k_{O3} = 6.2 \times 10^4$
259 M^{-1} s^{-1}) and the benzene ring (partly deactivated, $k_{O3} = 6.5 \times 10^3$ M^{-1} s^{-1}) (Lee et al., 2014).
260 This predicted k_{O3} of FRS is similar to the experimentally determined reactivity of compounds
261 with a p-sulfonylaniline moiety (Dodd et al., 2006). The QSAR model, however, did not
262 consider the reactivity of the furan ring, which explains why the k_{O3} determined
263 experimentally for FRS in this study ($k_{O3} = 2.2 \times 10^6$ M^{-1} s^{-1}) is significantly higher than the
264 value predicted by QSAR.

265

266 *3.2 Transformation of furans by ozone in water*

267 In addition to determining the ozonation kinetics of furans, the formation of transformation
268 products was investigated. Of particular interest was the formation of α,β-unsaturated
269 dicarbonyl compounds due to their potential toxicity and their recent identification in
270 oxidative water treatment processes (Prasse et al., 2018; Prasse et al., 2020). Ozonation
271 products were detected either directly with LC-HRMS, or after derivatization with either NAL
272 or a mixture of NAL and NAC (so called reactivity-directed analysis (RDA) assays) (Prasse,
273 2021). OH radicals were not scavenged in these experiments in order to represent real
274 ozonation conditions where both ozone and OH radicals are present.

275 *Transformation of furan-containing pharmaceuticals*. For FRS, seven ozonation products
276 were detected (Table S3 and Figure S11). The LC-HRMS results (exact mass, MS^2 spectra)
277 indicate that the benzene ring including the chlorine, sulfonamide and carboxyl moieties
278 remained unmodified in all ozonation products, which is in agreement with the deactivating
279 effect of these three benzene substituents. As such, oxidation of FRS can be attributed to the
280 reaction of ozone with the furfurylamine group, with FRS-278 being the only detected
281 compound that has been previously reported for the reaction with ozone (Aalizadeh et al.,
282 2019). Based on the obtained results, the reaction of ozone with the α-carbon of the furan
283 moiety is indicated to result in the opening of the furan ring (see section 3.3 for more details),
284 leading to the formation of an α,β-unsaturated dicarbonyl transformation product (FRS-347)
285 which has been observed previously in oxidation of FRS in microsomes (Williams et al.,
286 2007). The presence of an α,β-unsaturated dicarbonyl group is supported by the MS^2 spectrum
287 including the fragment m/z 262.9885 ($C_8H_8O_4N_2ClS$), which corresponds to cleavage of a
288 $C_4H_4O_2$ moiety. Formation of FRS-328, which has been identified in the oxidation of FRS by
289 dimethyldioxirane, can most likely be attributed to the intramolecular reaction between the
290 ketoenal group and the amine moiety of FRS-347 (Chen and Burka, 2007). The formation of
291 a ring condensation product is also supported by the absence of MS^2 fragments that indicate
292 cleavage of carbon-containing moieties. FRS-328 is also formed as a product of anodic and
293 electro-Fenton oxidation of FRS (Laurencé et al., 2011; Laurence et al., 2014), and has been
294 identified as a human metabolite of FRS with evidence that it is a physio-pathologically
295 relevant neurodegeneration inducer (Laurence et al., 2019). LC-HRMS results obtained for
296 FRS-265 show the presence of an additional methyl group compared to saluamine, an FRS
297 hydrolysis product (Cruz et al., 1979; Laurence et al., 2014). The formation of FRS-265 can
298 be explained by cleavage of the substituent on the α-carbon after furan ring opening. The

299 formation of the other transformation products can be explained by transformation of the furan

300 and secondary amine moieties, leading to carbonyls (FRS-308, FRS-363) and hydroxylamines

301 (FRS-266, FRS-308, FRS-363).

302 The chemical structures of the observed ozonation products suggest the relevance of two

303 reaction pathways involving the opening of the furan ring (Figure 1). The NAL assay was

304 used to assess whether α,β-unsaturated dicarbonyls (other than FRS-347) are formed from the

305 transformation of FRS. BDA was detected as a BDA-NAL adduct, indicating the relevance of

306 α,β-unsaturated dicarbonyl formation from the ozone oxidation of furan rings, even though

307 yields were low (< 0.1%). BDA and its substituted analogues have been identified as rat liver

308 microsomal metabolites of furan and furan containing compounds (Chen et al., 1995;

309 Peterson, 2013). The ozone dose-dependent formation of BDA and other FRS ozonation

310 products is shown in Figure S12.
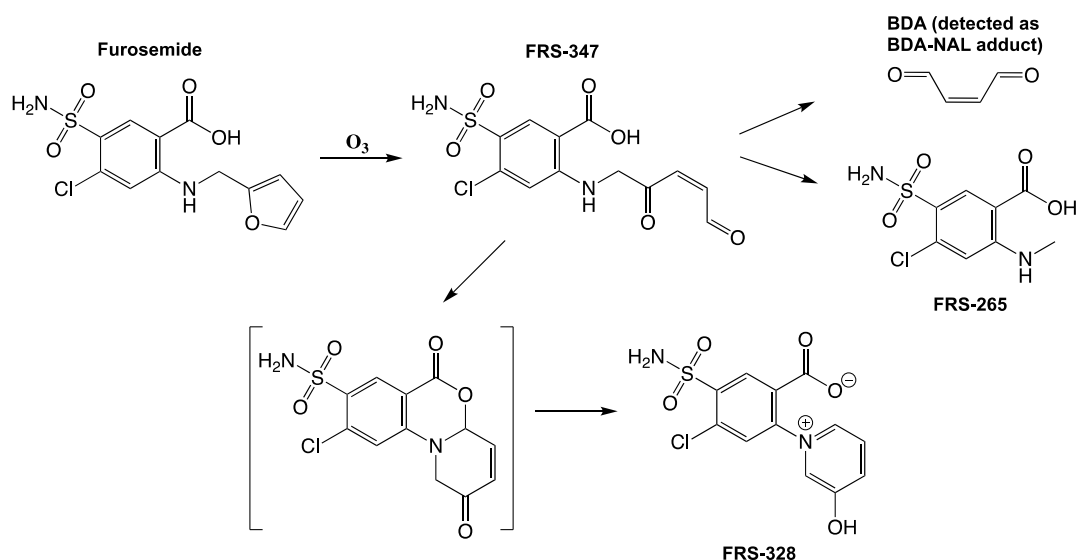
311

312 **Figure 1.** Proposed pathways of the ozonation of the furan ring of furosemide (FRS).

313

314 For RAN, twelve ozonation products were detected with two of them being formed by reaction

315 of ozone with the furan ring (Figures S13, S14, S15 and Table S4). Similar to results obtained

316 by Christophoridis et al. (2016), the LC-HRMS data indicate potential oxidation at different

317 positions of the molecule. However, in contrast to Christophoridis et al. (2016) who observed

318 only one ozonation product containing an additional oxygen atom ($C_{13}H_{22}N_4O_4S$) and

319 identified it as RAN-S oxide, two peaks with the same exact mass but distinct MS^2 spectra

320 were detected in the present study (Figure S14a and S14b). For the first peak (retention time:

321 3.7 min), the presence of MS^2 fragments m/z 188.0738 ($C_8H_{14}O_2NS$) and 192.0435

322 ($C_5H_{10}O_3N_3S$) indicates the oxidation of the thioether and thus the formation of the RAN-S

323   oxide. In contrast, the absence of both fragments in the MS^2 spectrum of the second peak

324   (retention time: 8.9 min) and the detection of fragment 270.0902 ($C_{11}H_{16}O_3N_3S$), which is

325   formed via cleavage of a C_2H_7ON group, suggests the oxidation of the tertiary amine group

326   and thus the formation of the RAN-N oxide. The formation of both N- and S-oxides is further

327   supported by the detection of RAN-S&N oxide ($C_{13}H_{22}N_4O_5S$) and the MS^2 results for this

328   compound (Figure S14c). The formation of other products also indicates the oxidation of the

329   tertiary amine group (Figure S14e and S14h). However, due to the absence of reference

330   standards, no final conclusions can be drawn. Transformation products formed during the

331   electrochemical oxidation of RAN have been shown to be more toxic than the parent

332   compound (Olvera-Vargas et al., 2014), emphasizing the need to elucidate the properties of

333   and the risk posed by the ozonation products of RAN.

334   Although all the RAN sub-structures react with ozone with high rates (Jeon et al., 2016), the

335   obtained results primarily demonstrated the formation of ozonation products in which the

336   furan ring remains unmodified. The detection of RAN-252 and RAN-236 also indicated the

337   oxidation of the furan moiety, leading to cleavage of parts of the molecule (Figure S14i and

338   S14j). However, it is possible that more ozonation products resulting from oxidation of the

339   furan ring were formed but could not be detected by LC-HRMS analysis. No α,β-unsaturated

340   dicarbonyl products were detected directly or after derivatization by NAL or a NAL+NAC

341   mixture, therefore dicarbonyls are either not formed from RAN or are degraded further.

342

343   *Ozonation products of substituted furans.* Based on the results of the furan-containing

344   pharmaceuticals, the formation of α,β-unsaturated dicarbonyls (BDA and BDA-Rs) from

345   simpler substituted furans was investigated to determine how different substituents impact the

346   formation of these toxic by-products. The results for seven tested compounds are summarised

347   in Table 2 and details are provided in the SI (Table S2 and Figures S4-S10). Concentrations

348   of BDA were determined using a reference standard. Due to the absence of reference

349   standards, the yields of BDA-Rs were determined by comparing the LC-HRMS peak areas of

350   their NAL adducts with those obtained for BDA.

351

352

353

354

Table 2. Maximum yield of α,β-unsaturated dicarbonyls in the aqueous ozonation of substituted furans, based on the detection of NAL, NAC and NAL+NAC adducts.

Compound	Substituents				Dicarbonyl formed	Max. yield (%)
	R_2	R_3	R_4	R_5		
DMF	$-CH_3$	$-H$	$-H$	$-CH_3$	$BDA(R_2)(R_5)$	Not quantified
FPA	$-C_2H_4COOH$	$-H$	$-H$	$-H$	BDA	<0.1
					BDA-R_2	2.7
MFA	$-CH_3$	$-COOH$	$-H$	$-H$	$BDA(R_2)(R_3)$	5.6
FFA	$-CH_2OH$	$-H$	$-H$	$-H$	BDA	2.4
					BDA-R_2	0.5
BHF	$-H$	$-CH_2OH$	$-CH_2OH$	$-H$	$BDA(R_3)(R_4)$	<0.1
FA	$-COOH$	$-H$	$-H$	$-H$	BDA	6.7
FDCA	$-COOH$	$-H$	$-H$	$-COOH$	-	-

The yields of BDA and BDA analogues were strongly dependent on the substituents present in different furans. Ozonation of FFA led to the formation of BDA at a maximum molar yield of 2.4 % (Figure 2). This is comparable to the BDA yields formed from UV/H_2O_2 oxidation of phenol in water (Prasse et al., 2018). Traces of BDA were also detected in the reaction solutions before the addition of ozone. This indicates the potential formation of BDA via hydrolysis of FFA, which aligns with previous reports on the acid-catalyzed hydrolysis of furans (Stamhuis et al., 1964). Besides BDA, a second C_4-dicarbonyl compound containing an additional hydroxymethyl group (NAL adduct $C_{13}H_{21}O_5N_2$, m/z 285.1444) was identified in experiments with FFA (BDA-R in Figure 2). The maximum relative yield of this compound was approximately 0.5%. The MS^2 spectrum of this adduct (Figure S5) contained characteristic masses (m/z 84.0813 and 126.0914) previously observed for NAL adducts of other dicarbonyls (Prasse et al., 2018). Ozonation of BHF did not lead to BDA formation, despite the structural similarity of BHF and FFA. However, the formation of a NAL adduct with m/z 315.1548 was detected in trace amounts, which can be attributed to the formation of a dialdehyde containing two hydroxymethyl substituents (Figure S6).
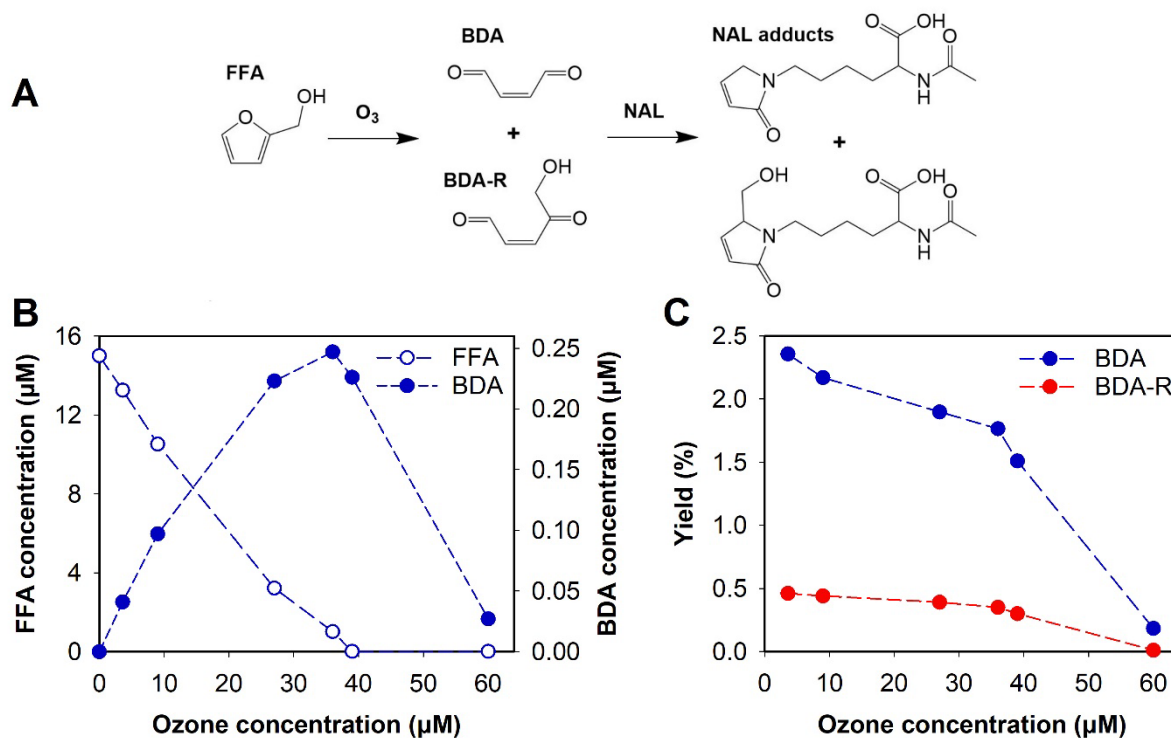
Figure 2. A. Chemical structures of furfuryl alcohol (FFA) and its dicarbonyl ozonation products based on the formation of NAL adducts. B. Concentration of FFA and 2-butene-1,4-dial (BDA) versus the ozone concentration. C. Molar yield of BDA and hydroxymethyl-BDA (BDA-R) determined by standard addition using a BDA reference standard. Conditions: FFA initial concentration 15 μM, in 10 mM phosphate buffer at pH 7.

BDA was also identified as an ozonation product of FA, at higher molar yields of approximately 7%, which was the maximum yield observed in this study. In comparison, chlorination of phenols has been shown to result in the formation of BDA-Rs at yields ranging from 18% to 46% (Prasse et al., 2020). No other NAL adducts were detected in FA experiments. For MFA, a BDA analogue with a carboxyl and a methyl group attached was detected (Figures 3 and S8), while ozonation of FPA led to formation of both BDA and a dicarbonyl with a propanoic acid group attached (Figures 3 and S7). The BDA molar yield was less than 0.1% in the case of FPA, while the propanoic acid-substituted BDA analogue appeared to be a more important ozonation product with a maximum yield of 2.7%. No NAL or NAC adducts were detected in ozonation of FDCA, in agreement with the results observed for RAN, indicating that the presence of two carboxyl substituents impacts both the reaction kinetics and the ozonation pathway.

392
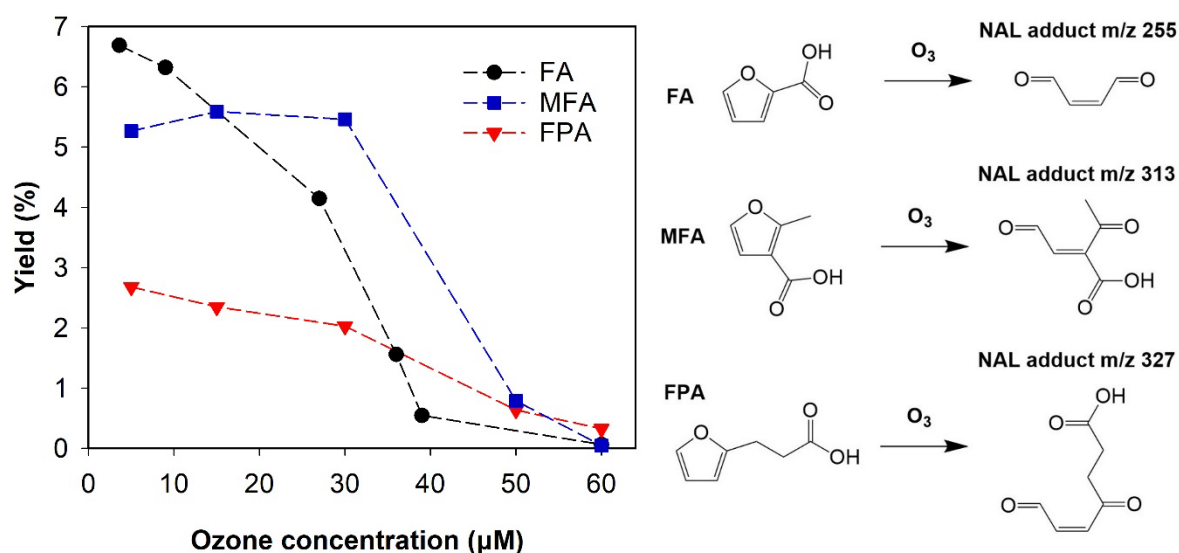
Figure 3. Molar yields of three α,β-unsaturated dicarbonyls formed in experiments with furan-containing acids at different ozone concentrations. Conditions: furan acid initial concentration 15 μM, in 10 mM phosphate buffer at pH 7. Yields were determined by standard addition using a 2-butene-1,4-dial (BDA) reference standard for all three compounds. For MFA, the ionization fragment m/z 269 was used for calculation of yields due to higher intensity.

The absence of a dimethylated BDA analogue in experiments with DMF can most likely be explained by the inability of this compound to react with NAL in the same way as the other dicarbonyl compounds detected, due to the presence of methyl substituents at both α-carbons. To verify this, additional experiments in the presence of both NAL and NAC were performed and revealed the formation of both NAC and NAL+NAC adducts (Figures S9 and S10). In contrast to NAL which primarily reacts with α,β-unsaturated dicarbonyl compounds via Schiff base formation (i.e. reaction at the carbonyl carbon), reactions of thiols can be attributed to Michael addition (i.e. reaction at the double bond adjacent to the carbonyl group) (LoPachin and Gavin, 2014). The formed thiol adducts can then react in a second step with NAL yielding pyrrole products (Figure S16).

The results demonstrate that α,β-unsaturated dicarbonyl compounds are relevant ozonation products of furans. The yields are generally low (< 7%), thus indicating the simultaneous formation of other ozonation products. In addition, the results show that BDA and BDA analogues can be transformed further by ozone (Figure S3). In the gas phase, BDA reacts with ozone with a rate constant of 1.6×10^{-18} cm^3 molecule^{-1} s^{-1} (Liu et al., 1999). Based on gas-phase ozonation studies of BDA and other related compounds, the products formed from the

415 further oxidation of BDA include formaldehyde, glyoxal and methylglyoxal (Liu et al., 1999;

416 Tuazon et al., 1985). These were not analysed in this study, but are the subject of ongoing

417 investigations.

418

419 *3.3 Postulated mechanism for the reaction of furans with ozone leading to α,β-unsaturated*

420 *dicarbonyls*

421 Even though no information is available about the transformation of furans by ozone in water,

422 previous studies performed in organic solvents have suggested the potential contribution of

423 different reaction mechanisms leading to opening of the furan ring (Bailey and Colomb, 1957;

424 Bailey et al., 1965; Jibben and Wibaut, 1960). Our detection of C_4 dicarbonyls (BDA

425 analogues) confirms the importance of electrophilic ozone attack at the reactive α-C positions

426 of the furan ring, via reaction of ozone with either one or both α-carbons (Figure 4) (Bailey,

427 1982). The yields of BDA and substituted BDA analogues, however, suggest ozonolysis of

428 furans via reaction with the α-β double bonds as dominant reaction pathway and/or further

429 reactions of the C_4 dicarbonyls with ozone.
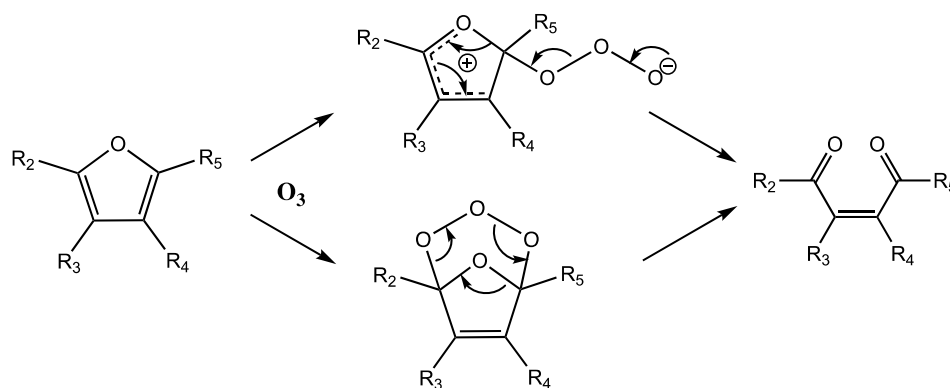
430

431 **Figure 4.** Postulated mechanism for the reaction of furans with ozone leading to formation of

432 2-butene-1,4-dial (BDA) and its analogues (BDA-Rs).

433

434 Similar to reaction kinetics, the obtained results further indicate that the yield and type of the

435 formed α,β-unsaturated dicarbonyls strongly depend on the substituents of the parent

436 compound and their position on the furan ring. Two of the tested compounds, MFA and BHF,

437 have substituents on the β-carbon of the furan ring (labelled as R_3 and R_4 in Tables 1 and 2).

438 Both the carboxyl group of MFA and the hydroxymethyl groups of BHF were retained on the

439 formed dicarbonyl compounds after ring opening (Table 2). The results of furans containing

440 substituents on the α-carbon (labelled as R_2 and R_5 in Tables 1 and 2) are less consistent. For

441 the ozonation of 2,5-diarylfurans in organic solvents, dicarbonyls containing aryl substituents
442 on both carbonyl carbons have been reported (Bailey et al., 1965; White et al., 1965). As
443 demonstrated in this study, a similar mechanism is also relevant under aqueous conditions for
444 MFA, FPA and DMF, all of which formed dicarbonyls with their α-C substituents still attached
445 (Table 2). This indicates that the reaction of ozone with furans containing alkyl substituents
446 on the α-carbon also results in the formation of BDA analogues with the substituents retained.
447 In contrast, results obtained for furans containing either hydroxymethyl or carboxylic acid
448 substituents at one of the α-carbons, indicate the relevance of reactions leading to cleavage of
449 the substituent and formation of BDA. This is particularly true for FA for which only the
450 formation of BDA but not BDA-R was observed. The differences in yield of BDA versus
451 BDA-R for FA, FFA and FPA reveal the significant influence of these α-C substituents on the
452 mechanism of BDA formation. FA is predominantly present as a carboxylate anion (pKa 3.0)
453 (Arena et al., 1993) under neutral pH, which is an electron-donating group, while the aldehyde
454 and alkene groups are electron-withdrawing. Thus, one of the potential explanations for BDA
455 formation during aqueous ozonation is through hydrolysis of the BDA-carboxylate yielding
456 (E)-4-hydroxybuta-1,3-dien-1-one as intermediate, which is unstable (Lin and Huang, 2018;
457 Yoshimi et al., 2010), and reacts further to BDA (Figure S17). Similar reaction mechanisms
458 leading to the removal of the hydroxymethyl and propanoic acid anion group can also be
459 postulated for FFA and FPA, respectively (Figure S17). Furthermore, the descending trend of
460 electron donating capacity from carboxylate anion to hydroxymethyl and propanoic acid
461 groups is in good agreement with the decreasing yield of BDA versus BDA-Rs. Differences
462 in the degradation of FFA and BDA in experiments performed in the presence and absence of
463 *tert*-butanol as a OH radical scavenger (Figure S3) were minor. However, the presence of *tert*-
464 butanol appeared to have some effect on the formed concentration of BDA and BDA-R
465 (Figure S2). The increased formation in the absence of *tert*-butanol indicates that BDA
466 analogues can be formed both from reactions with ozone and with OH radicals.

467

468 **4. Conclusions**

469 The selected organic compounds containing furan rings have a high ozone reactivity that is
470 comparable to that of activated benzene rings, and are therefore expected to be efficiently
471 eliminated in water and wastewater ozonation treatment. Further research is required to
472 elucidate the effect of deactivating substituents, such as halogens, on the ozonation rate
473 constant of furans.

In complex water matrices containing various furan-bearing compounds, ozonation is likely to result in the formation of a mixture of α,β-unsaturated dicarbonyls. Depending on the applied ozone dose, the dicarbonyls may decompose into smaller aldehydes and carboxylic acids. Future studies will focus on the detection of these further transformation products in real water treatment systems. In addition, it needs to be assessed whether α,β-unsaturated dicarbonyls can be removed during post-treatment steps, for example activated carbon and biofiltration.

The formation of α,β-unsaturated dicarbonyls such as BDA and its analogues, though only representing a small portion of transformation products from ozonation of furans, is a health concern due to their reported toxicity. Furans play an increasing role as 'green chemicals' and are also formed by natural processes in the aquatic environment. The obtained results highlight the necessity to investigate the fate of these compounds in water treatment systems to assess the potential exposures to toxic by-products.

495 **References**

496 Aalizadeh, R., Nika, M.C. and Thomaidis, N.S. (2019) Development and
497 application of retention time prediction models in the suspect and non-target
498 screening of emerging contaminants. J Hazard Mater 363, 277-285.

499 Arena, G., Cali, R., Maccarone, E. and Passerini, A. (1993) Thermodynamics of
500 protonation of some five-membered heteroaryl-carboxylates, -alkanoates and -
501 trans-propenoates. Journal of the Chemical Society, Perkin Transactions 2 (10),
502 1941-1945.

503 Bailey, P.S. (1982) Ozonation in Organic Chemistry. Bailey, P.S. (ed), pp. 111-
504 154, Academic Press.

505 Bailey, P.S. and Colomb, H.O. (1957) 1,4-ADDITION OF OZONE TO
506 FURANS AND PYRROLES. Journal of the American Chemical Society
507 79(15), 4238-4238.

508 Bailey, P.S., White, H.M. and Colomb, H.O. (1965) Ozonation of Diarylfurans.
509 The Journal of Organic Chemistry 30(2), 487-491.

510 Buxton, G.V., Greenstock, C.L., Helman, W.P. and Ross, A.B. (1988) Critical
511 Review of rate constants for reactions of hydrated electrons, hydrogen atoms
512 and hydroxyl radicals ($\cdot$OH/$\cdot$O$-$ in Aqueous Solution. Journal of Physical and
513 Chemical Reference Data 17(2), 513-886.

514 Chen, L.-J. and Burka, L.T. (2007) Chemical and Enzymatic Oxidation of
515 Furosemide: Formation of Pyridinium Salts. Chemical Research in Toxicology
516 20(12), 1741-1744.

517 Chen, L.-J., Hecht, S.S. and Peterson, L.A. (1995) Identification of cis-2-
518 Butene-1,4-dial as a Microsomal Metabolite of Furan. Chemical Research in
519 Toxicology 8(7), 903-906.

520 Christophoridis, C., Nika, M.C., Aalizadeh, R. and Thomaidis, N.S. (2016)
521 Ozonation of ranitidine: Effect of experimental parameters and identification of
522 transformation products. Sci Total Environ 557-558, 170-182.

523 Cruz, J.E., Maness, D.D. and Yakatan, G.J. (1979) Kinetics and mechanism of
524 hydrolysis of furosemide. International Journal of Pharmaceutics 2(5), 275-281.

525 Dodd, M.C., Buffle, M.-O. and von Gunten, U. (2006) Oxidation of
526 Antibacterial Molecules by Aqueous Ozone: Moiety-Specific Reaction

Kinetics and Application to Ozone-Based Wastewater Treatment. Environmental Science & Technology 40(6), 1969-1977.

Eldeeb, M. and Akih-Kumgeh, B. (2018) Recent Trends in the Production, Combustion and Modeling of Furan-Based Fuels. Energies 11(3), 512.

Gandini, A., Lacerda, T.M., Carvalho, A.J.F. and Trovatti, E. (2016) Progress of Polymers from Renewable Resources: Furans, Vegetable Oils, and Polysaccharides. Chemical Reviews 116(3), 1637-1669.

Gottschalk, C., Libra, J.A. and Saupe, A. (2009) Ozonation of water and waste water: A practical guide to understanding ozone and its applications, John Wiley & Sons.

Hannemann, K., Puchta, V., Simon, E., Ziegler, H., Ziegler, G. and Spiteller, G. (1989) The common occurrence of furan fatty acids in plants. Lipids 24(4), 296-298.

Hansch, C., Leo, A. and Taft, R.W. (1991) A survey of Hammett substituent constants and resonance and field parameters. Chemical Reviews 91(2), 165-195.

Huber, S.G., Wunderlich, S., Schöler, H.F. and Williams, J. (2010) Natural Abiotic Formation of Furans in Soil. Environmental Science & Technology 44(15), 5799-5804.

Hübner, U., von Gunten, U. and Jekel, M. (2015) Evaluation of the persistence of transformation products from ozonation of trace organic compounds – A critical review. Water Research 68, 150-170.

Jelic, A., Gros, M., Ginebreda, A., Cespedes-Sánchez, R., Ventura, F., Petrovic, M. and Barcelo, D. (2011) Occurrence, partition and removal of pharmaceuticals in sewage water and sludge during wastewater treatment. Water Research 45(3), 1165-1176.

Jeon, D., Kim, J., Shin, J., Hidayat, Z.R., Na, S. and Lee, Y. (2016) Transformation of ranitidine during water chlorination and ozonation: Moiety-specific reaction kinetics and elimination efficiency of NDMA formation potential. Journal of Hazardous Materials 318, 802-809.

557 Jibben, B.P. and Wibaut, J.P. (1960) The ozonisation and the ozonolysis of furan
558 and of some methylated furans in connection with the reactivities of the bonds
559 in the ringsystem. Recueil des Travaux Chimiques des Pays-Bas 79(4), 342-360.

560 Kasprzyk-Hordern, B., Dinsdale, R.M. and Guwy, A.J. (2008) The occurrence
561 of pharmaceuticals, personal care products, endocrine disruptors and illicit
562 drugs in surface water in South Wales, UK. Water Research 42(13), 3498-3518.

563 Keay, B.A. and Dibble, P.W. (1996) Comprehensive Heterocyclic Chemistry II.
564 Katritzky, A.R., Rees, C.W. and Scriven, E.F.V. (eds), pp. 395-436, Pergamon,
565 Oxford.

566 Kostich, M.S., Batt, A.L. and Lazorchak, J.M. (2014) Concentrations of
567 prioritized pharmaceuticals in effluents from 50 large wastewater treatment
568 plants in the US and implications for risk estimation. Environ Pollut 184, 354-
569 359.

570 Laurencé, C., Rivard, M., Lachaise, I., Bensemhoun, J. and Martens, T. (2011)
571 Preparative access to transformation products (TPs) of furosemide: a versatile
572 application of anodic oxidation. Tetrahedron 67(49), 9518-9521.

573 Laurence, C., Rivard, M., Martens, T., Morin, C., Buisson, D., Bourcier, S.,
574 Sablier, M. and Oturan, M.A. (2014) Anticipating the fate and impact of organic
575 environmental contaminants: a new approach applied to the pharmaceutical
576 furosemide. Chemosphere 113, 193-199.

577 Laurence, C., Zeghbib, N., Rivard, M., Lehri-Boufala, S., Lachaise, I., Barau,
578 C., Le Corvoisier, P., Martens, T., Garrigue-Antar, L. and Morin, C. (2019) A
579 new human pyridinium metabolite of furosemide, inhibitor of mitochondrial
580 complex I, is a candidate inducer of neurodegeneration. Biochemical
581 Pharmacology 160, 14-23.

582 Lee, M., Zimmermann-Steffens, S.G., Arey, J.S., Fenner, K. and von Gunten,
583 U. (2015) Development of Prediction Models for the Reactivity of Organic
584 Compounds with Ozone in Aqueous Solution by Quantum Chemical
585 Calculations: The Role of Delocalized and Localized Molecular Orbitals.
586 Environmental Science & Technology 49(16), 9925-9935.

587 Lee, Y., Kovalova, L., McArdell, C.S. and von Gunten, U. (2014) Prediction of
588 micropollutant elimination during ozonation of a hospital wastewater effluent.
589 Water Research 64, 134-148.

Lee, Y. and von Gunten, U. (2012) Quantitative structure–activity relationships (QSARs) for the transformation of organic micropollutants during oxidative water treatment. Water Research 46(19), 6177-6195.

Lee, Y. and von Gunten, U. (2016) Advances in predicting organic contaminant abatement during ozonation of municipal wastewater effluent: reaction kinetics, transformation products, and changes of biological effects. Environmental Science: Water Research & Technology 2(3), 421-442.

Lin, D.-Z. and Huang, J.-M. (2018) Electrochemical N-Formylation of Amines via Decarboxylation of Glyoxylic Acid. Organic Letters 20(7), 2112-2115.

Liu, X., Jeffries, H.E. and Sexton, K.G. (1999) Atmospheric Photochemical Degradation of 1,4-Unsaturated Dicarbonyls. Environmental Science & Technology 33(23), 4212-4220.

LoPachin, R.M. and Gavin, T. (2014) Molecular Mechanisms of Aldehyde Toxicity: A Chemical Perspective. Chemical Research in Toxicology 27(7), 1081-1091.

Mariscal, R., Maireles-Torres, P., Ojeda, M., Sádaba, I. and López Granados, M. (2016) Furfural: a renewable and versatile platform molecule for the synthesis of chemicals and fuels. Energy & Environmental Science 9(4), 1144-1189.

Olvera-Vargas, H., Oturan, N., Brillas, E., Buisson, D., Esposito, G. and Oturan, M.A. (2014) Electrochemical advanced oxidation for cold incineration of the pharmaceutical ranitidine: Mineralization pathway and toxicity evolution. Chemosphere 117, 644-651.

Peterson, L.A. (2013) Reactive metabolites in the biotransformation of molecules containing a furan ring. Chemical Research in Toxicology 26(1), 6-25.

Pohl, J., Golovko, O., Carlsson, G., Eriksson, J., Glynn, A., Orn, S. and Weiss, J. (2020) Carbamazepine Ozonation Byproducts: Toxicity in Zebrafish (Danio rerio) Embryos and Chemical Stability. Environ Sci Technol 54(5), 2913-2921.

Prasse, C. (2021) Reactivity-directed analysis – a novel approach for the identification of toxic organic electrophiles in drinking water. Environmental Science: Processes & Impacts.

622 Prasse, C., Ford, B., Nomura, D.K. and Sedlak, D.L. (2018) Unexpected
623 transformation of dissolved phenols to toxic dicarbonyls by hydroxyl radicals
624 and UV light. Proc Natl Acad Sci U S A 115(10), 2311-2316.

625 Prasse, C., von Gunten, U. and Sedlak, D.L. (2020) Chlorination of Phenols
626 Revisited: Unexpected Formation of α,β-Unsaturated C4-Dicarbonyl Ring
627 Cleavage Products. Environmental Science & Technology 54(2), 826-834.

628 Prasse, C., Wagner, M., Schulz, R. and Ternes, T.A. (2011) Biotransformation
629 of the antiviral drugs acyclovir and penciclovir in activated sludge treatment.
630 Environ Sci Technol 45(7), 2761-2769.

631 Ravindranath, V., Burka, L.T. and Boyd, M.R. (1984) Reactive metabolites
632 from the bioactivation of toxic methylfurans. Science 224(4651), 884.

633 Schlüter-Vorberg, L., Prasse, C., Ternes, T.A., Mückter, H. and Coors, A.
634 (2015) Toxification by Transformation in Conventional and Advanced
635 Wastewater Treatment: The Antiviral Drug Acyclovir. Environmental Science
636 & Technology Letters 2(12), 342-346.

637 Stamhuis, E.J., Drenth, W. and van den Berg, H. (1964) Mechanism of reactions
638 of furans I: A kinetic study of the acid-catalyzed hydrolysis of furan and 2,5-
639 dimethylfuran. Recueil des Travaux Chimiques des Pays-Bas 83(2), 167-176.

640 Tong, X., Ma, Y. and Li, Y. (2010) Biomass into chemicals: Conversion of
641 sugars to furan derivatives by catalytic processes. Applied Catalysis A: General
642 385(1), 1-13.

643 Tuazon, E.C., Atkinson, R. and Carter, W.P.L. (1985) Atmospheric chemistry
644 of cis- and trans-3-hexene-2,5-dione. Environmental Science & Technology
645 19(3), 265-269.

646 von Gunten, U. (2003) Ozonation of drinking water: Part I. Oxidation kinetics
647 and product formation. Water Research 37(7), 1443-1467.

648 von Gunten, U. (2018) Oxidation Processes in Water Treatment: Are We on
649 Track? Environ Sci Technol 52(9), 5062-5075.

650 von Sonntag, C. and von Gunten, U. (2012) Chemistry of ozone in water and
651 wastewater treatment, IWA publishing.

652 Wang, B., Wang, L., Li, Y. and Liu, Y. (2014) Heterocyclic terpenes: linear
653 furano- and pyrroloterpenoids. RSC Advances 4(24), 12216-12234.

654 White, H.M., Colomb, H.O. and Bailey, P.S. (1965) Ozonation of 2,5-
655 Diphenylfuran1. The Journal of Organic Chemistry 30(2), 481-486.

656 Williams, D.P., Antoine, D.J., Butler, P.J., Jones, R., Randle, L., Payne, A.,
657 Howard, M., Gardner, I., Blagg, J. and Park, B.K. (2007) The Metabolism and
658 Toxicity of Furosemide in the Wistar Rat and CD-1 Mouse: a Chemical and
659 Biochemical Definition of the Toxicophore. Journal of Pharmacology and
660 Experimental Therapeutics 322(3), 1208-1220.

661 Yoshimi, Y., Kobayashi, K., Kamakura, H., Nishikawa, K., Haga, Y., Maeda,
662 K., Morita, T., Itou, T., Okada, Y. and Hatanaka, M. (2010) Addition of alkyl
663 radicals, generated from carboxylic acids via photochemical decarboxylation, to
664 glyoxylic oxime ether: a mild and efficient route to α-substituted α-aminoesters.
665 Tetrahedron Letters 51(17), 2332-2334.

666 Zou, R., Liao, X., Zhao, L. and Yuan, B. (2018) Reduction of N-
667 nitrosodimethylamine formation from ranitidine by ozonation preceding
668 chloramination: influencing factors and mechanisms. Environ Sci Pollut Res Int
669 25(14), 13489-13498.

670 Zoumpouli, G.A., Siqueira Souza, F., Petrie, B., Féris, L.A., Kasprzyk-Hordern,
671 B. and Wenk, J. (2020) Simultaneous ozonation of 90 organic micropollutants
672 including illicit drugs and their metabolites in different water matrices.
673 Environmental Science: Water Research & Technology 6(9), 2465-2478.

674

TOC art
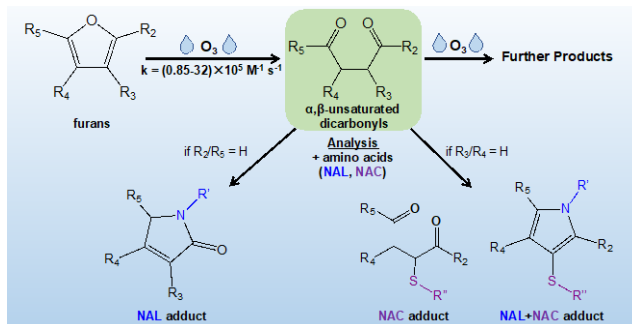
Supplementary Information

Aqueous Ozonation of Furans: Kinetics and Transformation Mechanisms Leading to the Formation of α,β-Unsaturated Dicarbonyl Compounds

Garyfalia A. Zoumpouli[a,b,c,d,1], Zhuoyue Zhang[d], Jannis Wenk[b,c], and Carsten Prasse[d,*]

[a] Centre for Doctoral Training, Centre for Sustainable Chemical Technologies, University of Bath, Bath BA2 7AY, UK.

[b] Department of Chemical Engineering, University of Bath, Bath BA2 7AY, UK.

[c] Water Innovation and Research Centre (WIRC), University of Bath, Bath BA2 7AY, UK.

[d] Department of Environmental Health and Engineering, Johns Hopkins University, Baltimore, MD 21218, USA.

[*] corresponding author. Email: cprasse1@jhu.edu; Address: 3400 N Charles Street, Baltimore, MD 21218

[1] Present address: Cranfield Water Science Institute, Cranfield University, College Road, Cranfield MK43 0AL, UK

Content

Tables

Figures

concentration 15 μM, *tert*-butanol concentration 10 mM, in 10 mM phosphate buffer at pH 7.

Supplementary text S1: ozonation experiments

The competition kinetics experiments were performed in 20-mL amber glass vials. The reaction solutions (10 or 15 mL) contained 7 μM of the target compound, 7 μM of the reference compound (RAN or FA), 10 mM phosphate buffer (pH 7) and 10 mM *tert*-butanol in ultrapure

water. Ozone stock solution was added to achieve concentrations of 1 to 13 μM ozone (0.1 to 0.9 μM O_3/μM target plus reference compound). Samples were magnetically stirred during the addition of the ozone stock solution and then left overnight at room temperature until complete ozone depletion. Residual concentrations of the target and reference compounds were measured within 24 hours. The second order rate constant for the reaction of the target compound with ozone ($k_{O3,TC}$) was calculated from the plot of the natural logarithm of the relative concentration of target compound versus the natural logarithm of the relative concentration of reference compound (see Figure S1), according to the equation (Huber et al., 2003):

$$\ln\left(\frac{[TC]}{[TC]_0}\right) = \frac{k_{O_3,TC}}{k_{O_3,RC}}\ln\left(\frac{[RC]}{[RC]_0}\right)$$

The ± error of each rate constant was calculated through error propagation from the 95% confidence interval of the slope of the linear fit and the estimated error of $k_{O3,\ RAN}$ (± 0.1×10^6 M^{-1} s^{-1}) (Jeon et al., 2016) or the calculated error of $k_{O3,\ FA}$.

To prepare the concentrated ozone stock solution for either batch ozonation experiments or competition kinetics, two different systems were used. One was a 500-mL glass reactor that was equipped with a gas diffuser and a water jacket, with the temperature of the recirculating water in the jacket set to 2°C. The other was a 1-L glass bottle placed in an ice bath. Both systems were fed with oxygen containing 50 to 100 mg/L ozone, produced with either a BMT 803N ozone generator (Messtechnik GmbH) or an IOCS integrated ozone system (Pacific Ozone). The dissolved ozone concentration of the ozone stock solution (20 to 30 mg/L) was measured spectrophotometrically both before and after its addition into the reaction solutions, either directly at 258 nm (molar absorptivity of ozone ε=2900 M^{-1} cm^{-1}) or with the indigo method (Bader and Hoigné, 1981).

Supplementary text S2: liquid chromatography-high resolution mass spectrometry

For chromatographic separation the gradient program was at 75 μL/min with ultrapure water containing 0.1 % formic acid (A) and methanol (B). The percentage of A was: 0-3 min, 100%; 3-12 min, linear decrease from 100% to 5%; 12-14 min, 5%; 14.1 min, 100%, total run time 20 min. The injection volume was 10 μL.

The Electrospray ionization (ESI) source parameters were set as follows. Sheath gas flow rate: 20 arbitrary units (AU); aux gas flow rate: 10 AU; spray voltage: 3.8 kV for positive mode and 2.5 kV for negative mode; capillary temperature: 250°C; S-lens RF level: 60; aux gas

heater temperature: 100°C. Data-dependent acquisition was used to conduct MS^2 experiments. Full scan (50-700 m/z, resolution > 120000) was performed followed by data-dependent MS^2 for the 5 most intense ions with resolution > 60000. Collision induced dissociation (CID) with stepped normalized collision energy of 10%, 30% and 50% was used for fragmentation with an isolation window of 1.0 m/z.

Table S1. HPLC-UV parameters for the detection of furans in competition kinetics experiments. Flow rate 0.5 mL/min, A: ultrapure water with 0.1 % v/v formic or phosphoric acid, B: acetonitrile.

Compound	A/B (%/%)	Retention time (min)	Detection wavelength (nm)
Furfuryl alcohol (FFA)	90/10	2.9	216
2-Furoic acid (FA)	90/10	3.3	252
2-Methyl-3-furoic acid (MFA)	70/30	2.6	245
3-(2-Furyl)propanoic acid (FPA)	70/30	2.9	220
Furosemide (FRS)	60/40	3.0	228
Ranitidine (RAN)	90/10	2.2	320
Furan-2,5-dicarboxylic acid (FDCA)	90/10	2.5	265
3,4-Bis(hydroxymethyl)furan (BHF)	90/10	1.8	215

Table S2. NAL, NAC and NAL+NAC adducts detected in this study with LC-HRMS.

| Parent compound	Amino acid added	Adduct m/z (observed)	m/z error (ppm)	Adduct formula $[M+H]^+$	Dicarbonyl formula
FFA, FA, FPA, FRS	NAL	255.1338	-0.39	$C_{12}H_{19}O_4N_2$	$C_4H_4O_2$
FFA	NAL	285.1444	-0.35	$C_{13}H_{21}O_5N_2$	$C_5H_6O_3$
FPA	NAL	327.1549	-0.61	$C_{15}H_{23}O_6N_2$	$C_7H_8O_4$
MFA	NAL	313.1391	-0.96	$C_{14}H_{21}O_6N_2$	$C_6H_6O_4$
BHF	NAL	315.1548	-0.95	$C_{14}H_{23}O_6N_2$	$C_6H_8O_4$
DMF	NAC	276.0899	-0.36	$C_{11}H_{18}O_5NS$	$C_6H_8O_2$
DMF	NAL+NAC	428.1852	0.48	$C_{19}H_{30}O_6N_3S$	$C_6H_8O_2$
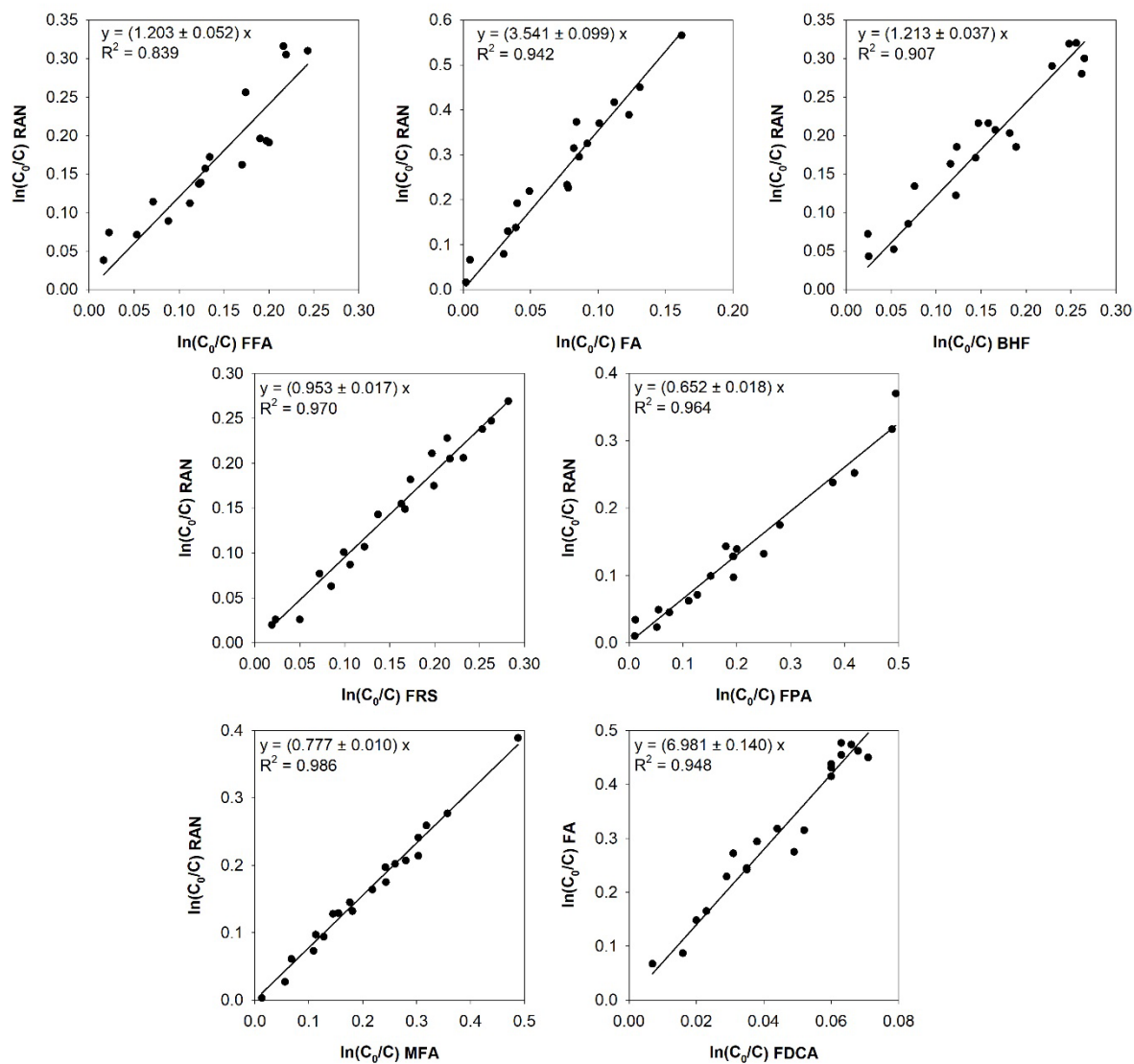
Figure S1. Plot of the natural logarithm of the relative concentration of the reference compound (RAN or FA) versus the natural logarithm of the relative concentration of the target compound (FFA, FA, FRS, FPA, MFA, BHF, FDCA). Linear fit equations are shown including the standard error of the slope.
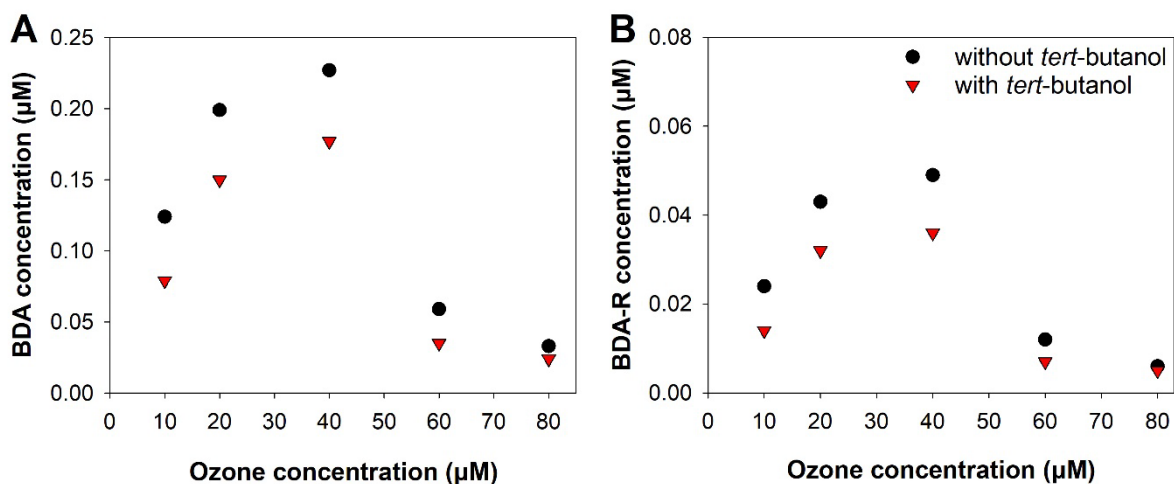
Figure S2. Effect of *tert*-butanol addition on the formation of BDA and BDA-R (hydroxymethyl-BDA) during the ozonation of FFA. FFA initial concentration 15 μM, *tert*-butanol concentration 10 mM, in 10 mM phosphate buffer at pH 7.
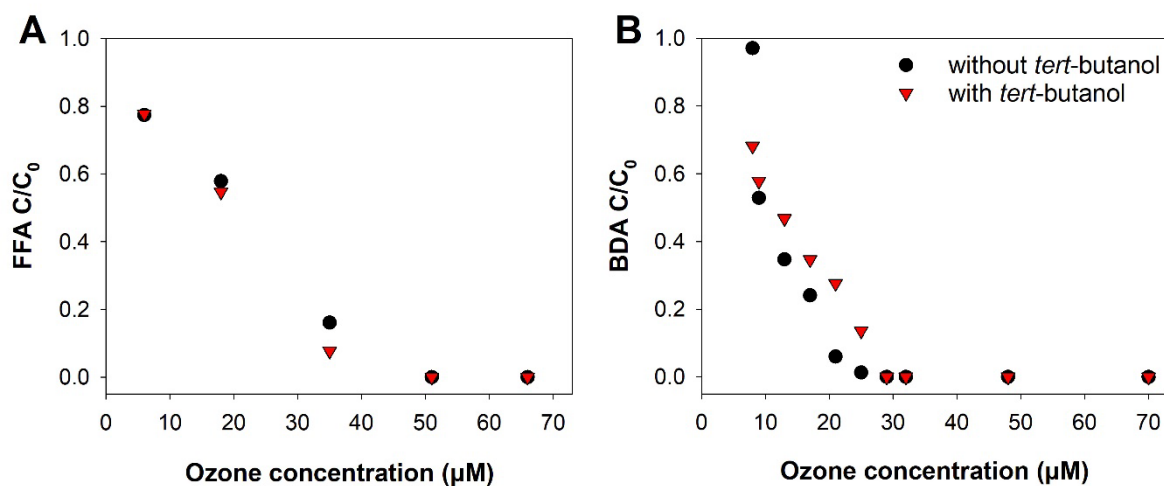
Figure S3. Degradation of A) FFA and B) BDA at different ozone concentrations, with or without addition of 10 mM *tert*-butanol, in 10 mM phosphate buffer at pH 7.
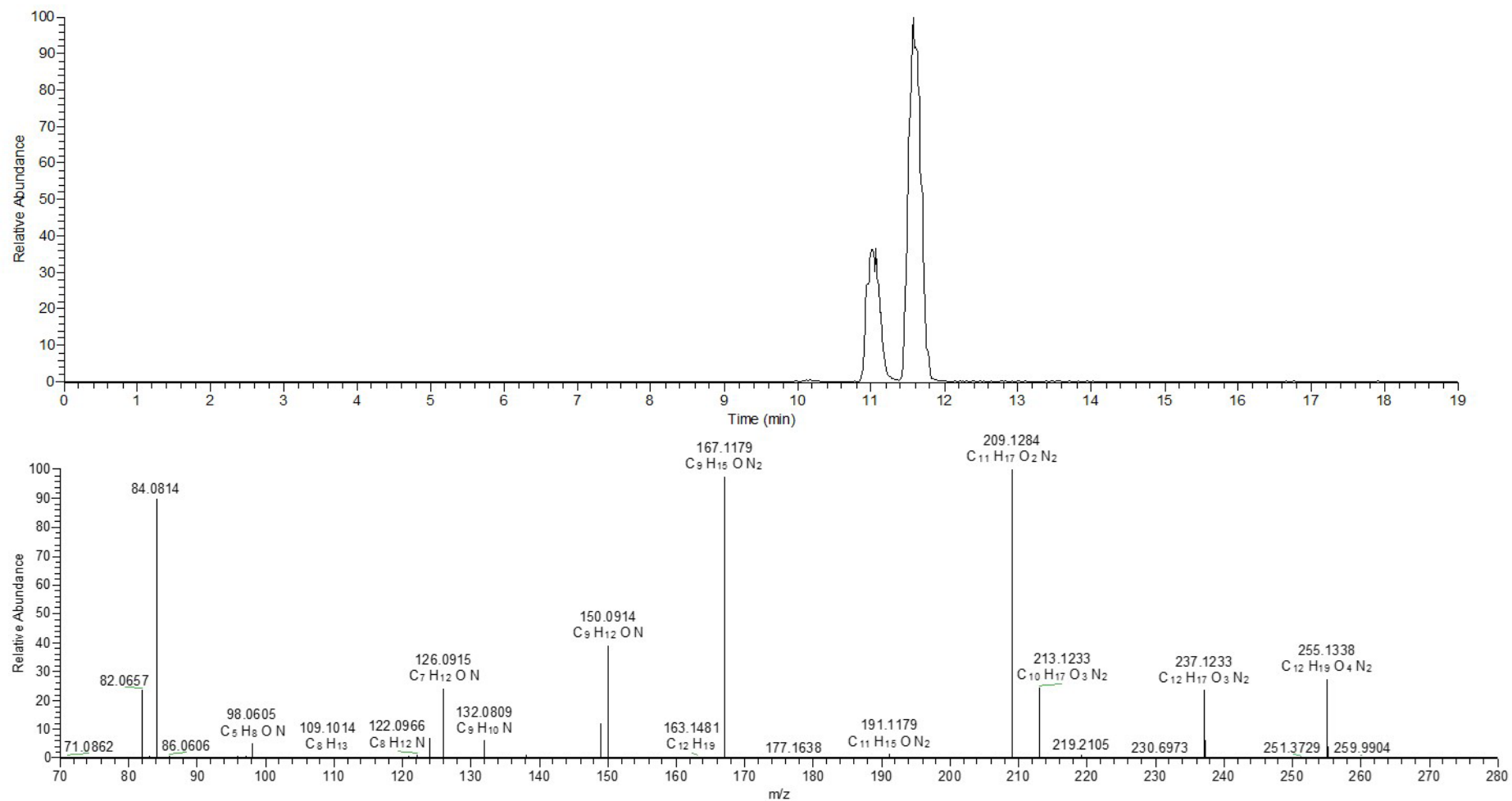
Figure S4. Base peak chromatogram and MS^2 spectrum of m/z 255 (NAL adduct of BDA) identified in ozonation experiments with furfuryl alcohol (15 μM initial concentration).
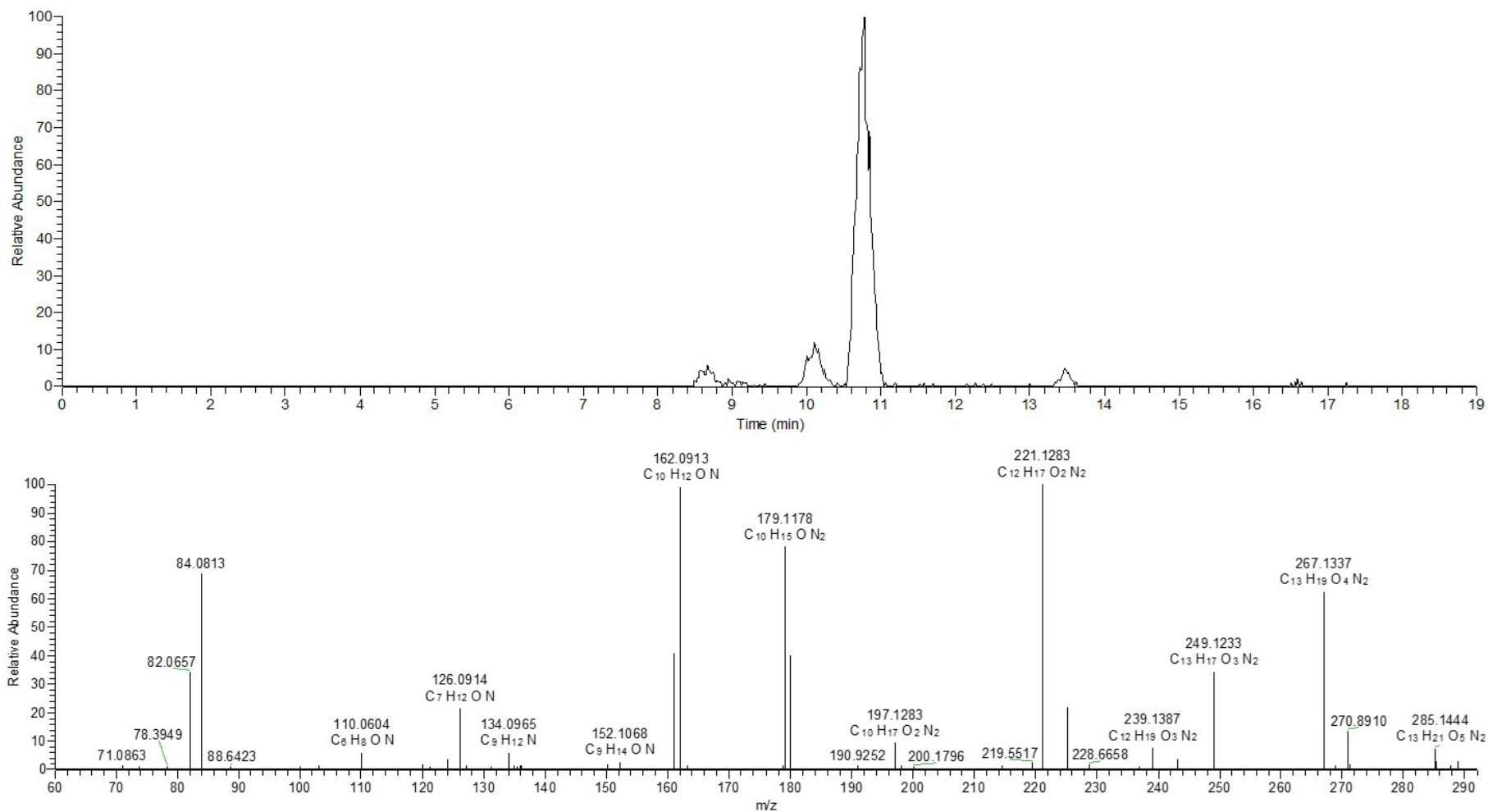
Figure S5. Base peak chromatogram and MS^2 spectrum of m/z 285 identified in ozonation experiments with furfuryl alcohol (15 μM initial concentration).
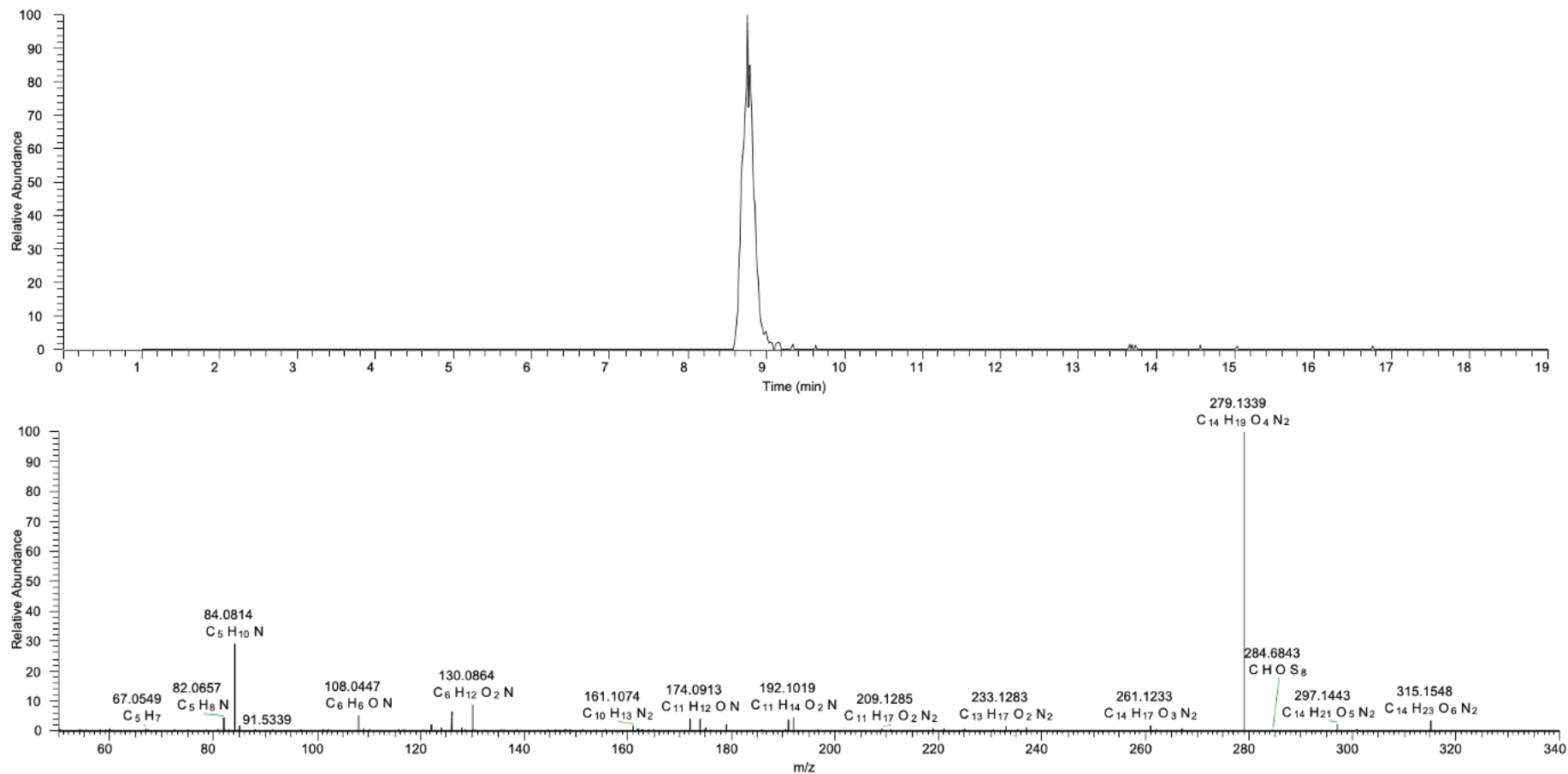
Figure S6. Base peak chromatogram and MS^2 spectrum of m/z 315 identified in ozonation experiments with 3,4-bis(hydroxymethyl)furan (100 μM initial concentration).
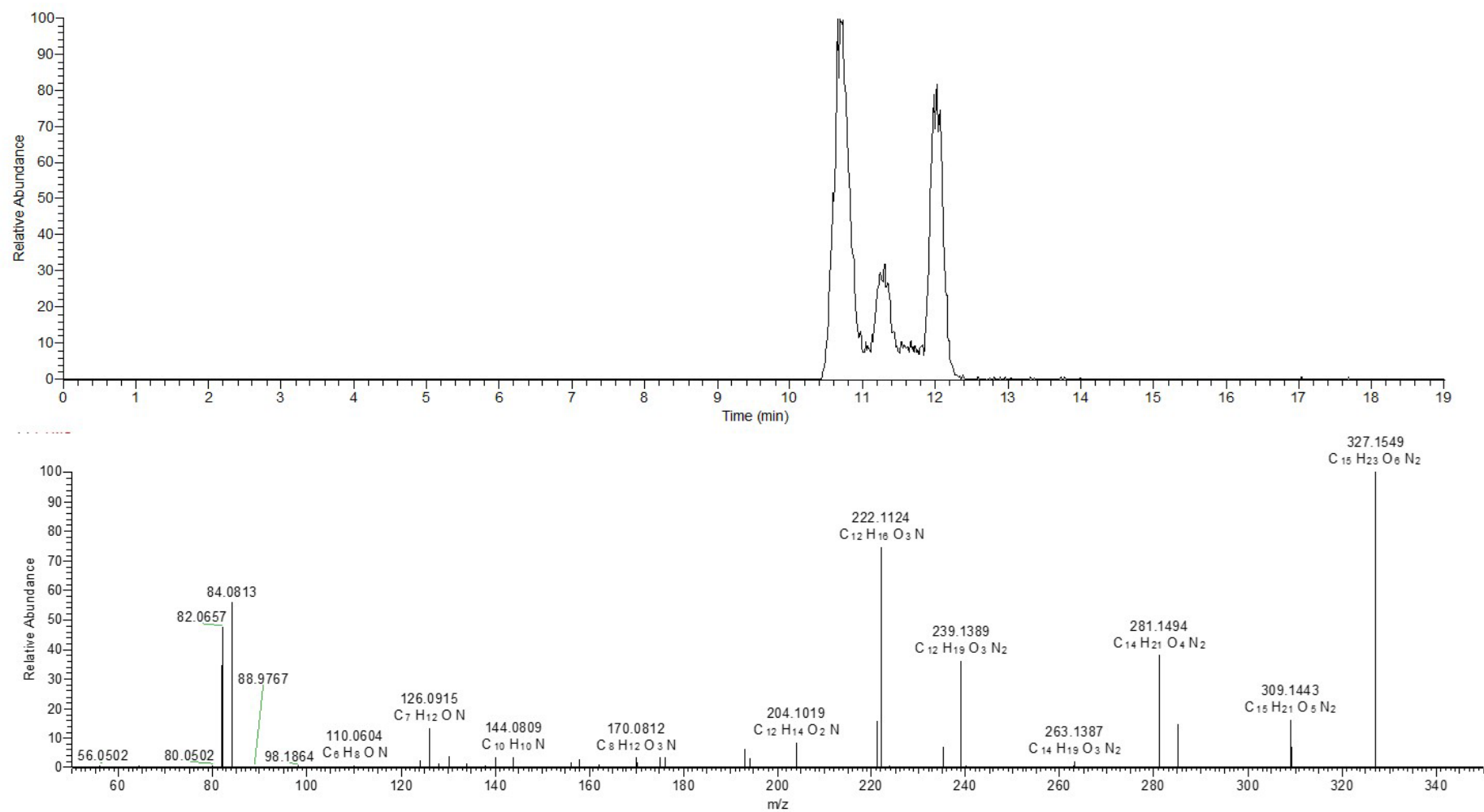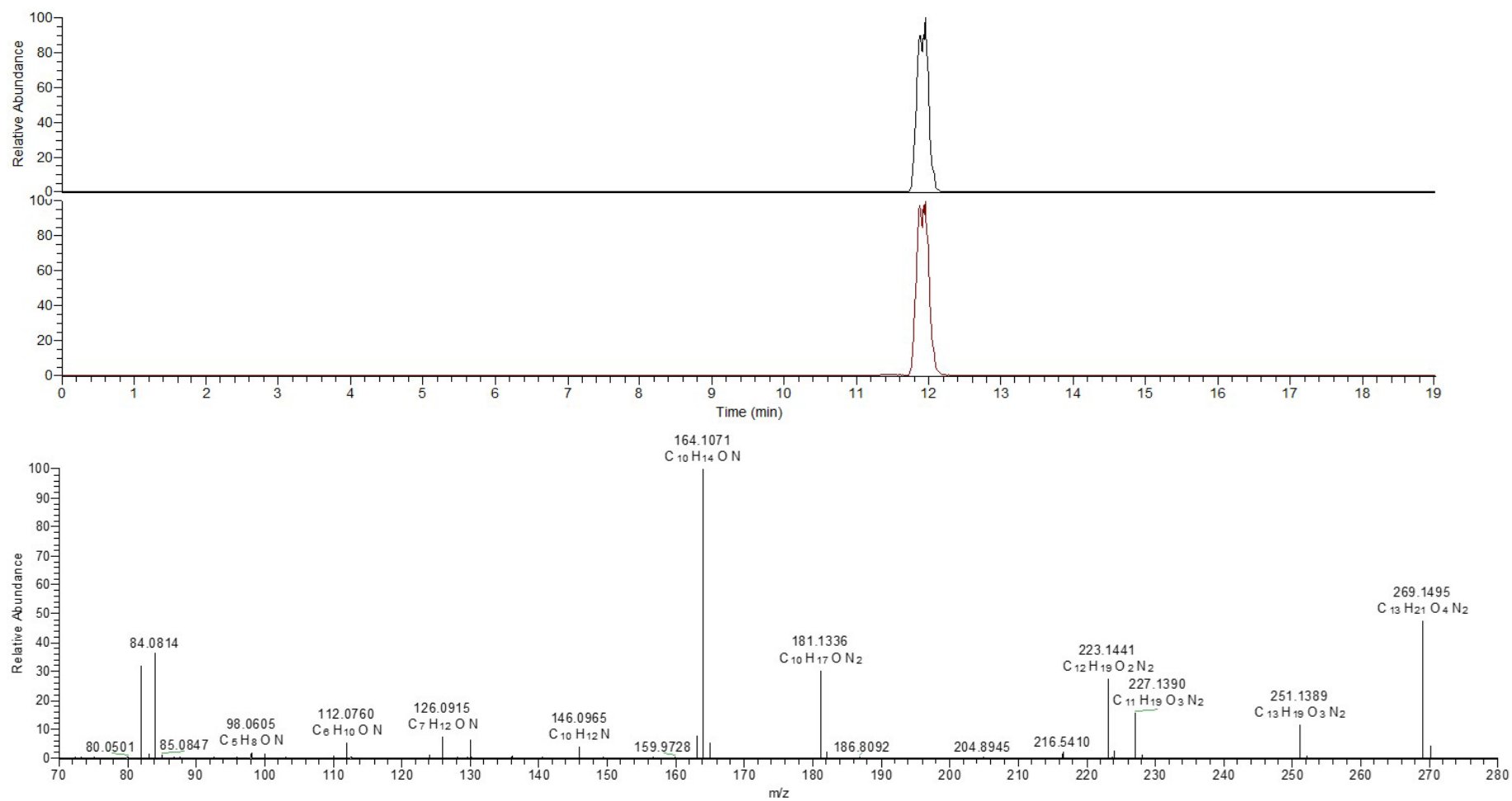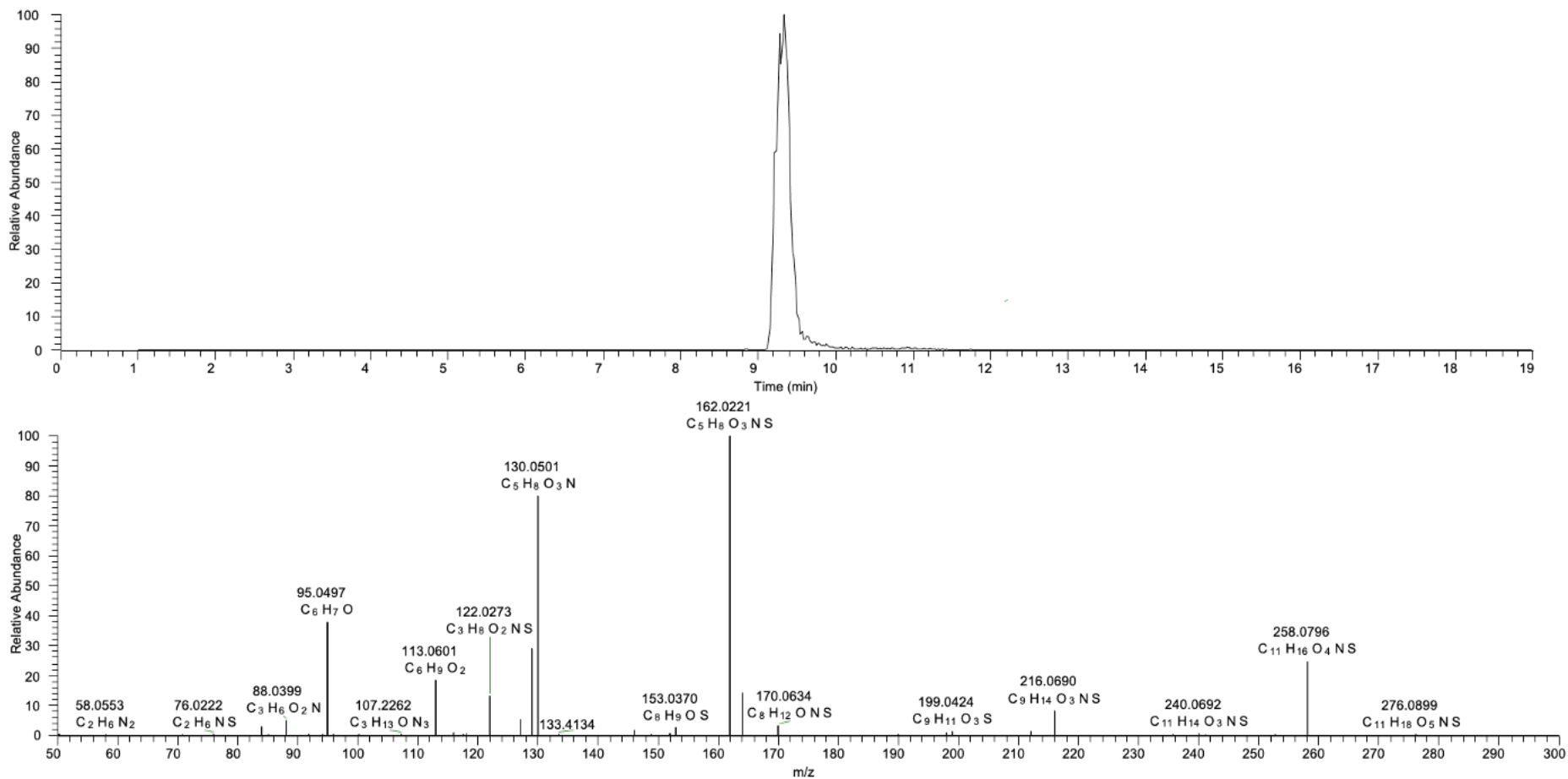
Figure S7. Base peak chromatogram and MS^2 spectrum of m/z 327 identified in ozonation experiments with 3-(2-furyl)propanoic acid (15 μM initial concentration).

Figure S8. Base peak chromatogram of m/z 313 (top), base peak chromatogram and MS^2 spectrum of m/z 269 (m/z 313 after loss of CO_2) identified in ozonation experiments with 2-methyl-3-furoic acid (15 µM initial concentration).

Figure S9. Base peak chromatogram and MS^2 spectrum of m/z 276 identified in ozonation experiments with 2,5-dimethylfuran (100 μM initial concentration).
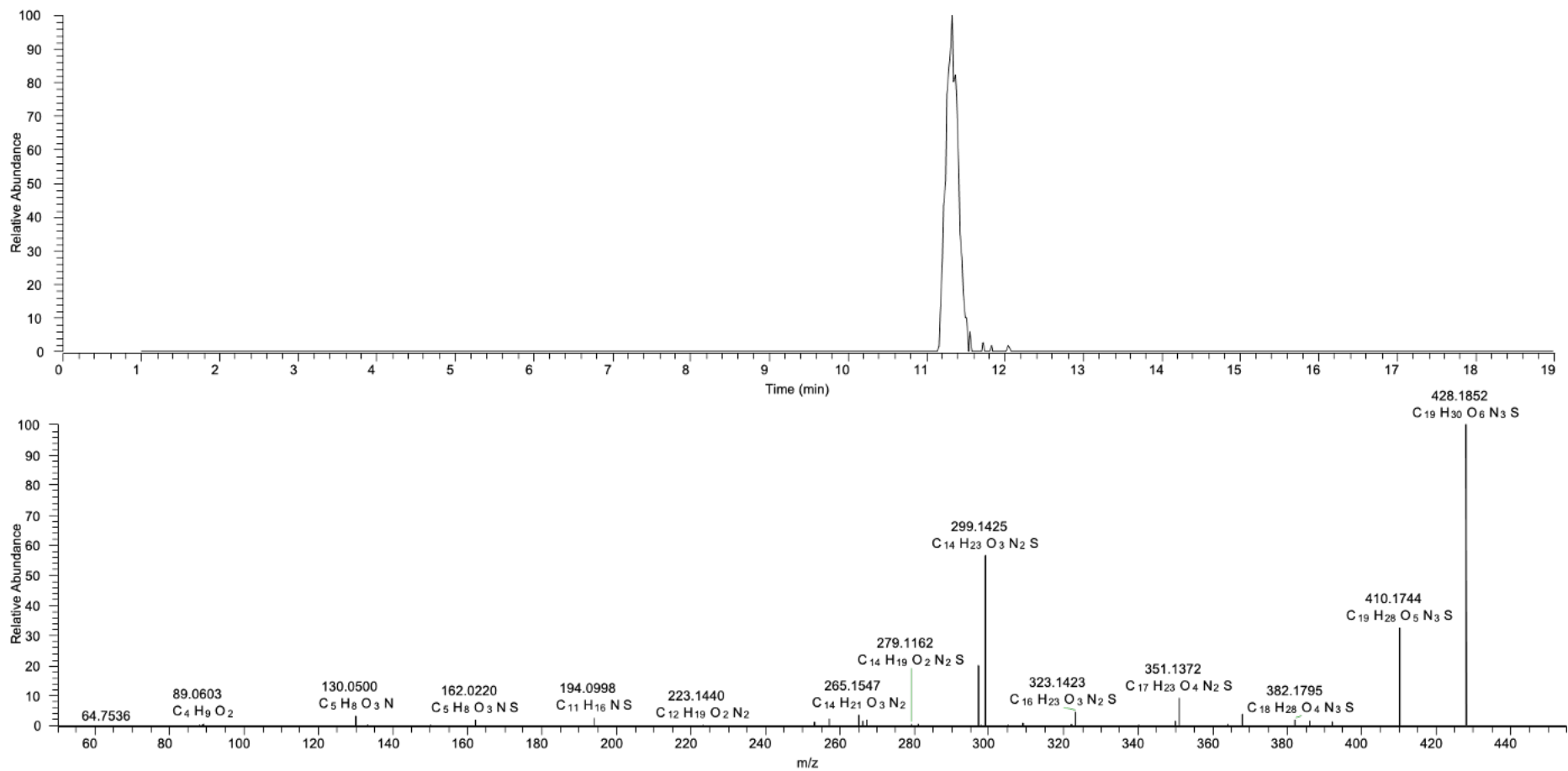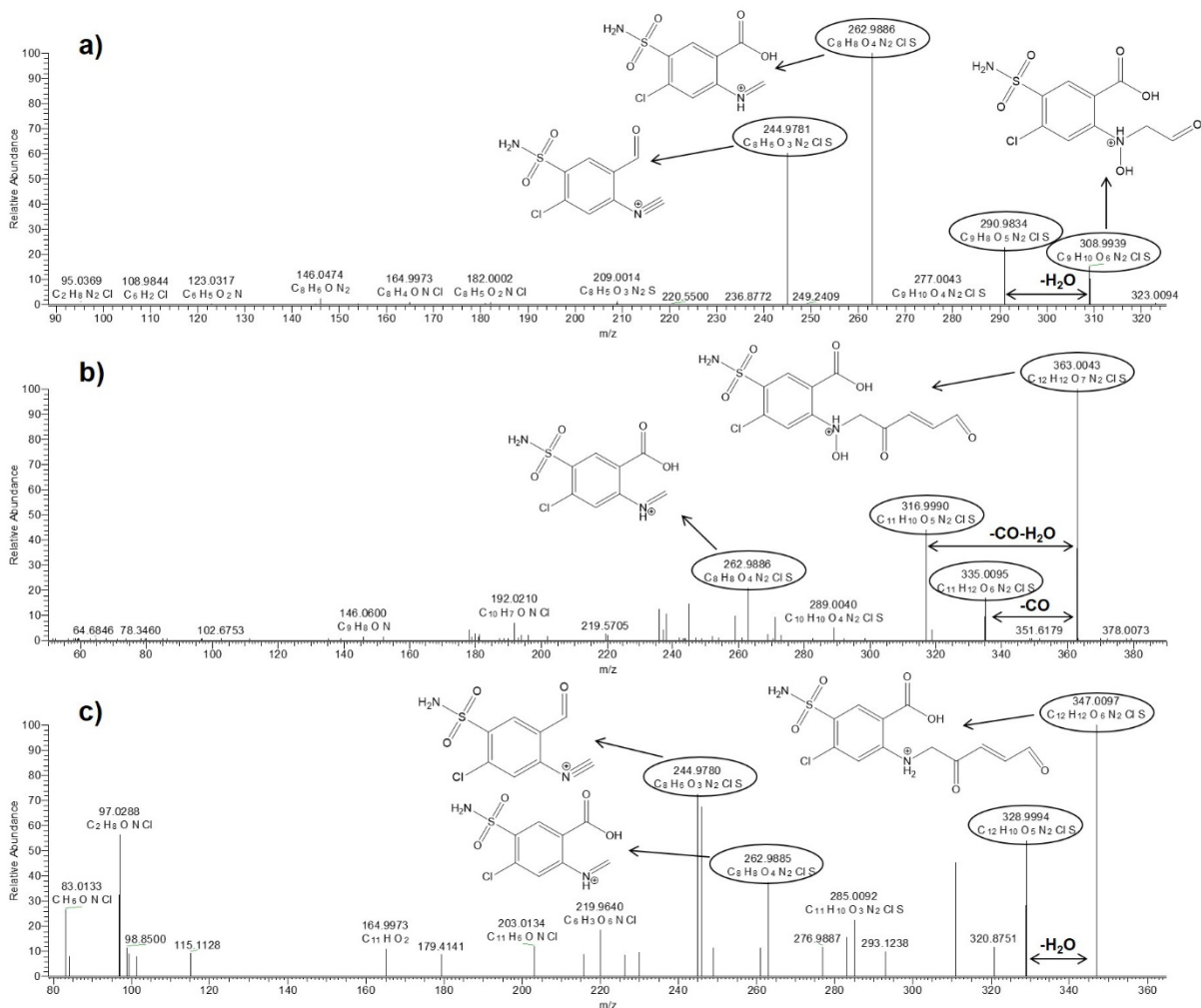
Figure S10. Base peak chromatogram and MS^2 spectrum of m/z 428 identified in ozonation experiments with 2,5-dimethylfuran (100 μM initial concentration).

Table S3. Furosemide ozonation products detected with LC-HRMS, including MS^2 fragmentation information. Suggested structures are supported by comparison with literature (Aalizadeh et al., 2019; Laurence et al., 2014), and/or based on MS^2 spectra (Figure S11).

Compound	Retention time (min)	m/z (observed)	m/z error (ppm)	Formula [M+H]$^+$	Suggested structure
FRS	14.1	331.0143 250.9885 232.9780 185.9951	2.1 1.1 0.9 0.8	$C_{12}H_{12}O_5N_2ClS$ $C_7H_8O_4N_2ClS$ $C_7H_6O_3N_2ClS$ $C_7H_5O_3NCl$	
FRS-265	11.1	265.0042 250.9886 232.9782 185.9952	0.9 0.7 0.1 0.3	$C_8H_{10}O_4N_2ClS$ $C_7H_8O_4N_2ClS$ $C_7H_6O_3N_2ClS$ $C_7H_5O_3NCl$	
FRS-328	8.0	328.9989 310.9880 281.0082 266.0211 249.0184	1.4 2.5 1.3 1.4 1.3	$C_{12}H_{10}O_5N_2ClS$ $C_{12}H_8O_4N_2ClS$ $C_{12}H_8O_5NCl$ $C_{12}H_9O_4NCl$ $C_{12}H_8O_3NCl$	
FRS-308	12.0	308.9939 290.9834 262.9886 244.9781	1.2 1.0 0.7 0.5	$C_9H_{10}O_6N_2ClS$ $C_9H_8O_5N_2ClS$ $C_8H_8O_4N_2ClS$ $C_8H_6O_3N_2ClS$	
FRS-363 (two peaks)	9.1, 10.0	363.0043 335.0095 316.9990 262.9886	1.4 1.2 1.1 0.7	$C_{12}H_{12}O_7N_2ClS$ $C_{11}H_{12}O_6N_2ClS$ $C_{11}H_{10}O_5N_2ClS$ $C_8H_8O_4N_2ClS$	
FRS-347	11.8	347.0097 328.9994 262.9885 244.9780	0.6 -0.2 1.1 0.9	$C_{12}H_{12}O_6N_2ClS$ $C_{12}H_{10}O_5N_2ClS$ $C_8H_8O_4N_2ClS$ $C_8H_6O_3N_2ClS$	
FRS-266	10.6	266.9834 248.9729	1.1 0.9	$C_7H_8O_5N_2ClS$ $C_7H_6O_4N_2ClS$	
FRS-278	11.8	278.9834	1.1	$C_8H_8O_5N_2ClS$	

Figure S11. MS^2 spectra including fragment structures for the newly detected products a) FRS-308, b) FRS-363 and c) FRS-347 identified in ozonation experiments with furosemide (15 μM initial concentration).
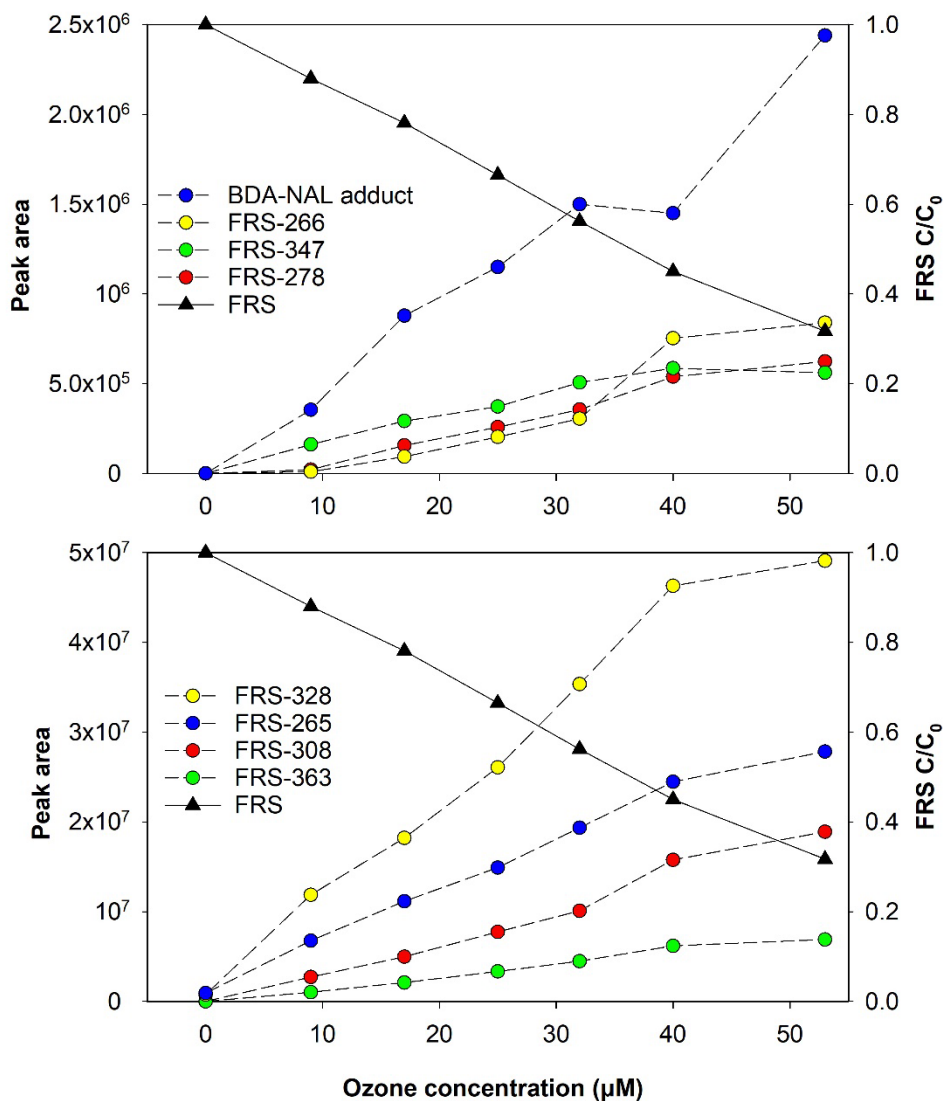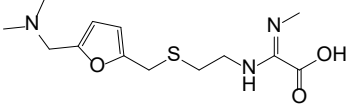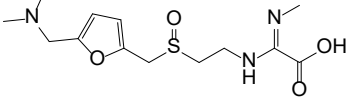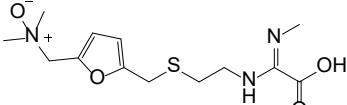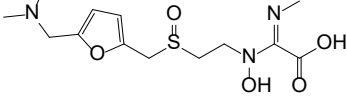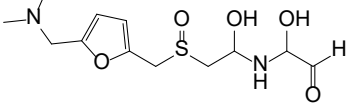
Figure S12. Peak area of furosemide (FRS) ozonation products and FRS degradation at different ozone concentrations. BDA is shown as the BDA-NAL adduct. For FRS-265 the peak area of the ionisation fragment m/z 250 is shown. Data points are the average of duplicate experiments (error bars have been omitted). Furosemide initial concentration 15 μM.
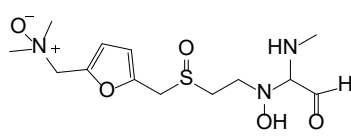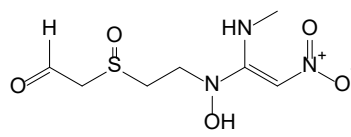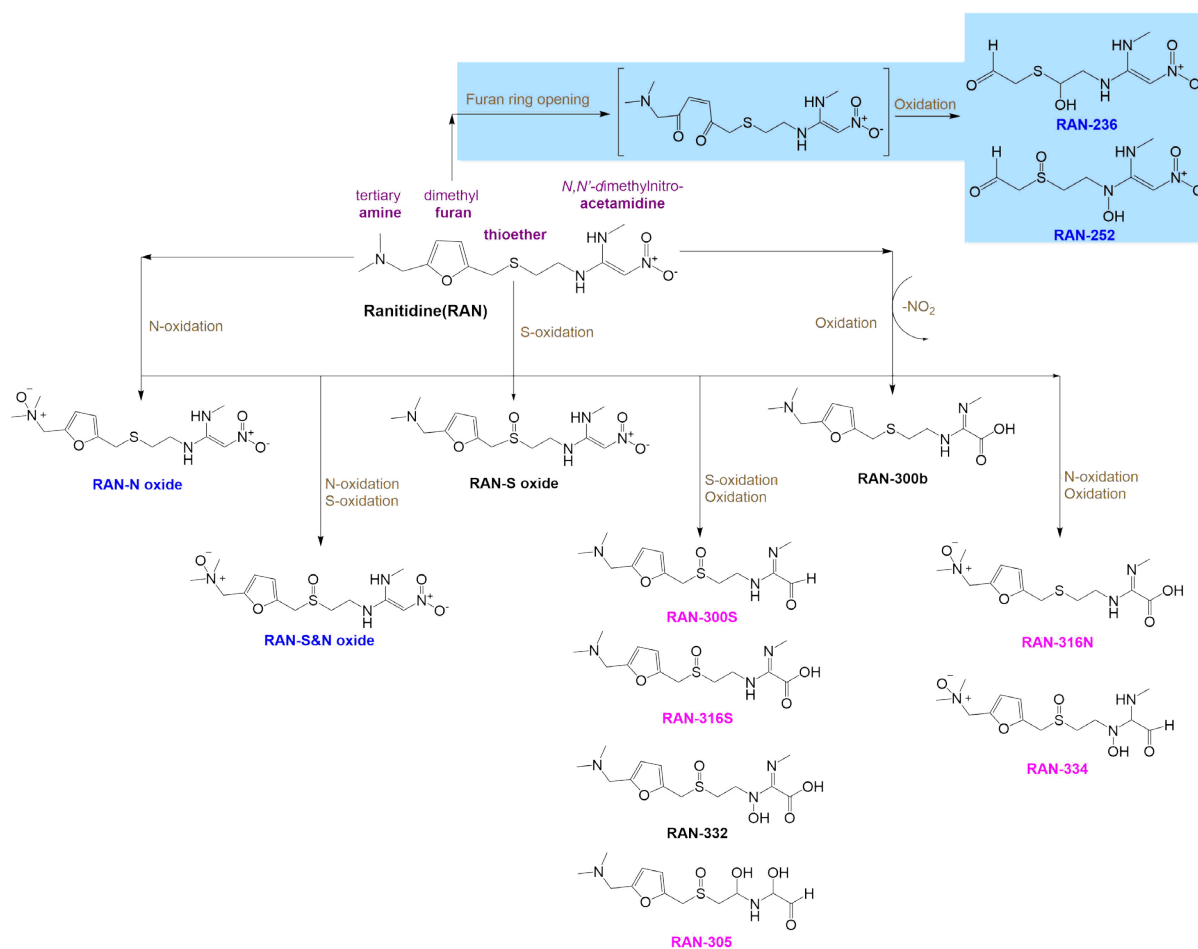
Table S4. Ranitidine ozonation products detected with LC-HRMS, including MS^2 fragmentation information. Suggested structures are supported by comparison with literature (Christophoridis et al., 2016), and/or based on MS^2 spectra (Figure S14).

Compound	Retention time (min)	m/z (observed)	m/z error (ppm)	Formula [M+H]$^+$	Suggested structure
RAN	8.7	315.1481	-1.5	$C_{13}H_{23}O_3N_4S$	
		270.0902	-1.8	$C_{11}H_{16}O_3N_3S$	
		224.0974	-1.6	$C_{11}H_{16}ON_2S$	
		176.0487	-0.8	$C_5H_{10}O_2N_3S$	
		144.0766	-1.2	$C_5H_{10}O_2N_3$	
		124.0757	0.2	$C_7H_{10}ON$	
		117.0481	0.2	$C_4H_9N_2S$	
		98.0842	3.1	$C_5H_{10}N_2$	
		58.0658	11.0	C_3H_8N	
RAN-S oxide	3.7	331.1430	-1.3	$C_{13}H_{23}O_4N_4S$	
		313.1330	0.4	$C_{13}H_{21}O_3N_4S$	
		286.0851	-1.9	$C_{11}H_{16}O_4N_3S$	
		240.0924	-1.3	$C_{11}H_{16}O_2N_2S$	
		222.0818	-1.4	$C_{11}H_{14}ON_2S$	
		192.0435	-1.5	$C_5H_{10}O_3N_3S$	
		188.0738	-1.1	$C_8H_{14}O_2NS$	
		138.0913	-0.2	$C_8H_{12}ON$	
		110.0967	2.0	$C_7H_{12}N$	
		94.0417	3.5	C_6H_6O	
		82.0656	6.1	C_5H_8N	
		58.0658	11.0	C_3H_8N	
RAN-N oxide	8.9	331.1429	-1.8	$C_{13}H_{23}O_4N_4S$	
		270.0902	-1.7	$C_{11}H_{16}O_3N_3S$	
		224.0974	-1.7	$C_{11}H_{16}ON_2S$	
		176.0486	-1.0	$C_5H_{10}O_2N_3S$	
		144.0766	-1.2	$C_5H_{10}O_2N_3$	
		130.0559	1.2	$C_5H_{10}N_2S$	
		98.0842	3.2	$C_5H_{10}N_2$	
		88.0220	4.7	C_3H_6NS	
RAN-S&N oxide	4.2	347.1379	-1.7	$C_{13}H_{23}O_5N_4S$	
		286.0850	-2.0	$C_{11}H_{16}O_4N_3S$	
		240.0920	-2.7	$C_{11}H_{16}O_2N_2S$	
		193.0513	-1.4	$C_5H_{11}O_3N_3S$	
		192.0434	-1.7	$C_5H_{10}O_3N_3S$	
		146.0506	-1.6	$C_5H_{10}ON_2S$	
		130.0610	-1.1	$C_4H_8O_2N_3$	
		100.0998	2.5	$C_5H_{12}N_2$	
		73.0765	7.0	$C_3H_9N_2$	
RAN-300S	2.0	300.1371	-1.6	$C_{13}H_{22}O_3N_3S$	
		282.1266	-1.6	$C_{13}H_{20}O_2N_3S$	
		255.0793	-2.0	$C_{11}H_{15}O_3N_2S$	
		237.0687	-2.0	$C_{11}H_{13}O_3N_2S$	

		m/z	ppm	Formula	Structure
		188.0737	-1.5	$C_8H_{14}O_2NS$	
		138.0913	-0.3	$C_8H_{12}ON$	
		110.0966	1.8	$C_7H_{12}N$	
		94.0416	3.5	C_6H_6O	
		82.0656	6.1	C_5H_8N	
		58.0658	11.0	C_3H_8N	
RAN-300b	6.0	300.1369	-2.5	$C_{13}H_{22}O_3N_3S$	
		256.1473	-2.1	$C_{12}H_{22}ON_3S$	
		211.0896	-1.9	$C_{10}H_{15}ON_2S$	
		170.0631	-1.9	$C_8H_{12}ONS$	
		153.0366	-1.9	C_8H_9OS	
		138.0911	-1.4	$C_8H_{12}ON$	
		125.0055	-0.8	C_6H_5OS	
		124.0757	-0.2	$C_7H_{10}ON$	
		117.0481	0.4	$C_4H_9N_2S$	
		85.0764	4.8	$C_4H_9N_2$	
RAN-316S	2.3	316.1320	-1.8	$C_{13}H_{22}O_4N_3S$	
		272.1423	-1.7	$C_{12}H_{22}O_2N_3S$	
		254.1317	-1.8	$C_{12}H_{20}ON_3S$	
		227.0845	-1.7	$C_{10}H_{15}O_2N_2S$	
		209.0741	-0.9	$C_{10}H_{13}ON_2S$	
		188.0738	-1.1	$C_8H_{14}O_2NS$	
		138.0912	-0.7	$C_8H_{12}ON$	
		110.0966	1.7	$C_7H_{12}N$	
		85.0765	5.4	$C_4H_9N_2$	
		58.0658	11.0	C_3H_8N	
RAN-316N	7.2	316.1317	-2.8	$C_{13}H_{22}O_4N_3S$	
		272.1421	-2.3	$C_{12}H_{22}O_2N_3S$	
		212.0973	-2.2	$C_{10}H_{16}ON_2S$	
		170.0631	-1.7	$C_8H_{12}ONS$	
		153.0365	-2.4	C_8H_9OS	
		118.0559	0.1	$C_4H_{10}N_2S$	
		85.0764	4.7	$C_4H_9N_2$	
RAN-332	4.0	332.1270	-1.4	$C_{13}H_{22}O_5N_3S$	
		288.1372	-1.5	$C_{12}H_{22}O_3N_3S$	
		243.0795	-1.3	$C_{10}H_{15}O_3N_2S$	
		227.0847	-0.8	$C_{10}H_{15}O_2N_2S$	
		151.0534	-0.9	$C_4H_{11}O_2N_2S$	
		149.0378	-0.9	$C_4H_9O_2N_2S$	
		138.0912	-0.8	$C_8H_{12}ON$	
		134.0508	-0.5	$C_4H_{10}ON_2S$	
		110.0966	1.4	$C_7H_{12}N$	
		85.0765	5.2	$C_4H_9N_2$	
RAN-305	2.2	305.1159	-2.1	$C_{12}H_{21}O_5N_2S$	
		287.1054	-2.0	$C_{12}H_{19}O_4N_2S$	
		166.0165	-2.0	$C_4H_8O_4NS$	
		138.0912	-1.1	$C_8H_{12}NO$	
		110.0966	1.5	$C_7H_{12}N$	
		94.0417	4.3	C_6H_6O	

RAN-334	2.2	334.1426 316.1317 255.0790 180.0558 177.0326 162.0456 161.0375 113.0710 95.0494	-1.4 -2.8 -3.0 -1.8 -1.1 -1.2 -2.4 0.1 2.4	$C_{13}H_{24}O_5N_3S$ $C_{13}H_{22}O_4N_3S$ $C_{11}H_{15}O_3N_2S$ $C_5H_{12}O_3N_2S$ $C_5H_9O_3N_2S$ $C_5H_{10}O_2N_2S$ $C_5H_9O_2N_2S$ $C_5H_9ON_2$ C_6H_7O	
RAN-236	7.5	236.0697 219.0670 190.0768 131.0638 119.0163 73.0112	-1.2 -1.2 -1.6 0.0 1.1 8.1	$C_7H_{14}O_4N_3S$ $C_7H_{13}O_3N_3S$ $C_7H_{14}O_2N_2S$ $C_5H_{11}N_2S$ $C_4H_7O_2S$ C_3H_5S	
RAN-252	2.4	252.0645 234.0540 206.0719 193.0518 188.0612 176.0251 160.0299 144.0766 134.0270 98.0842	-1.3 -1.4 -0.1 1.2 -1.0 0.5 -1.1 -1.0 -0.5 3.5	$C_7H_{14}O_5N_3S$ $C_7H_{12}O_4N_3S$ $C_7H_{14}O_3N_2S$ $C_5H_{11}O_3N_3S$ $C_7H_{12}O_2N_2S$ $C_5H_8O_3N_2S$ $C_5H_8O_2N_2S$ $C_5H_{10}O_2N_3S$ $C_4H_8O_2NS$ $C_5H_{10}N_2$	

19

Figure S13. Proposed reaction pathways for the ozonation of ranitidine. Transformation products are labelled as follows: blue ones are newly detected, black ones are previously reported (Christophoridis et al., 2016), while pink ones are those having the same molecular ion m/z as previously reported (Christophoridis et al., 2016), but different suggested structures based on MS^2 fragment information obtained (Figure S14).
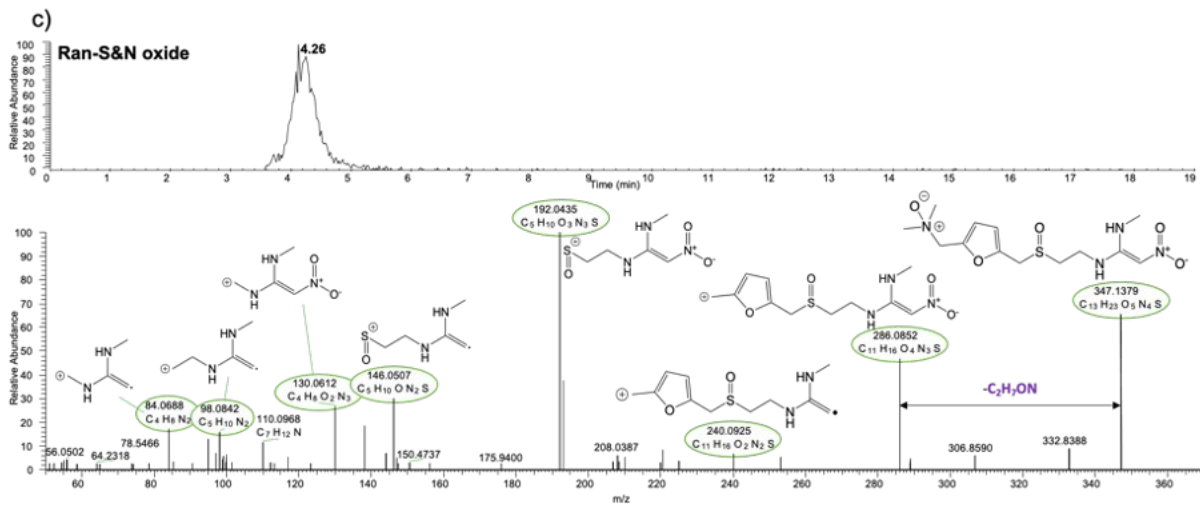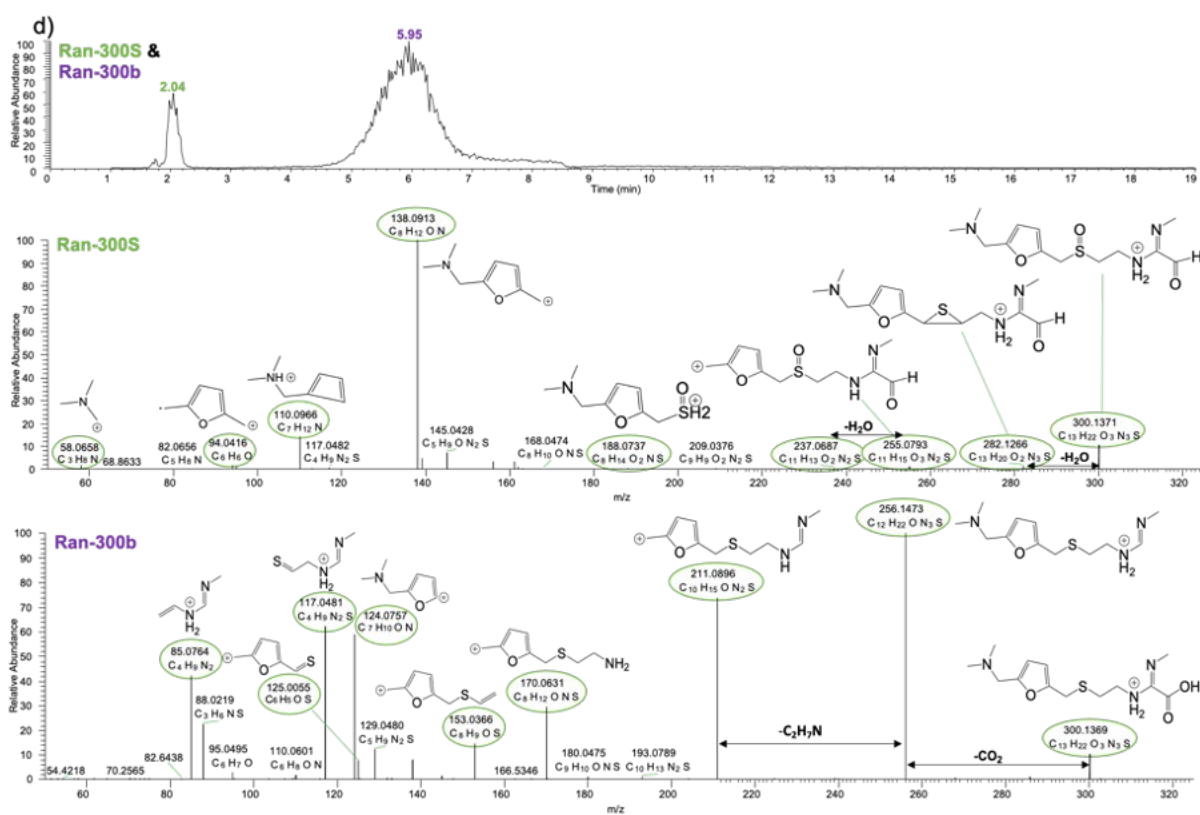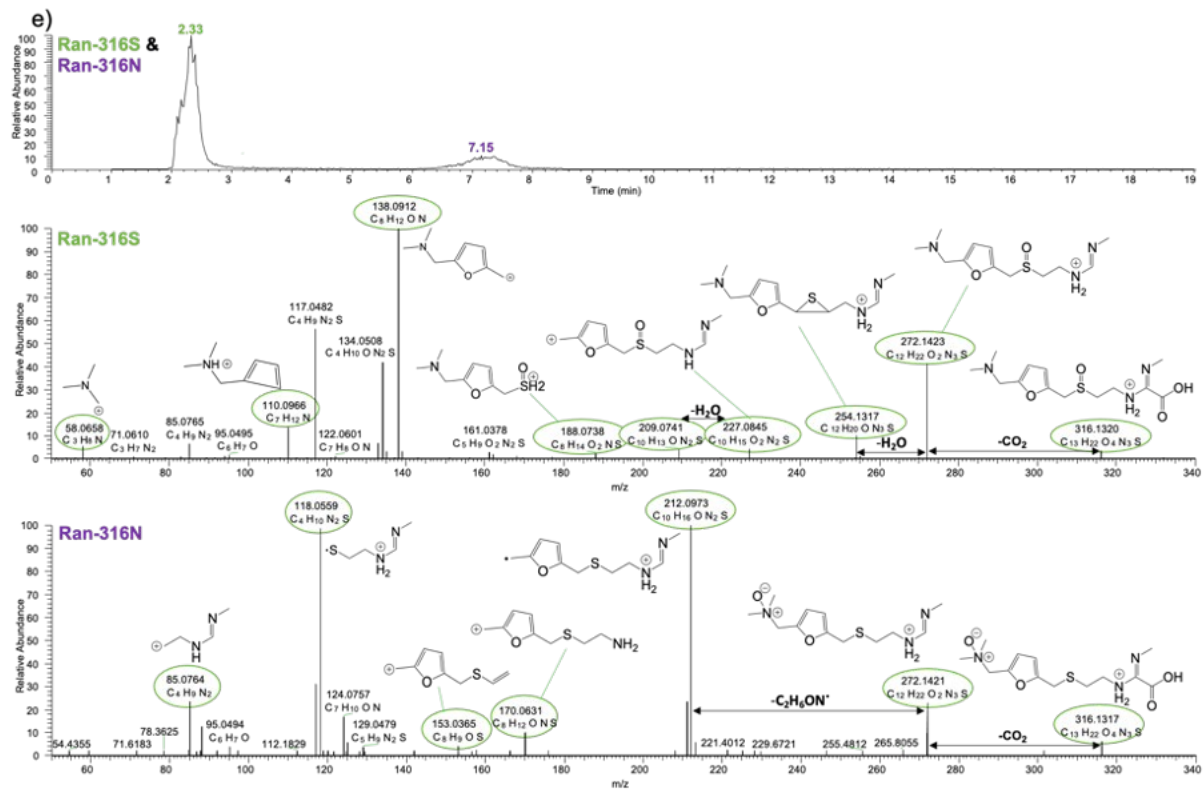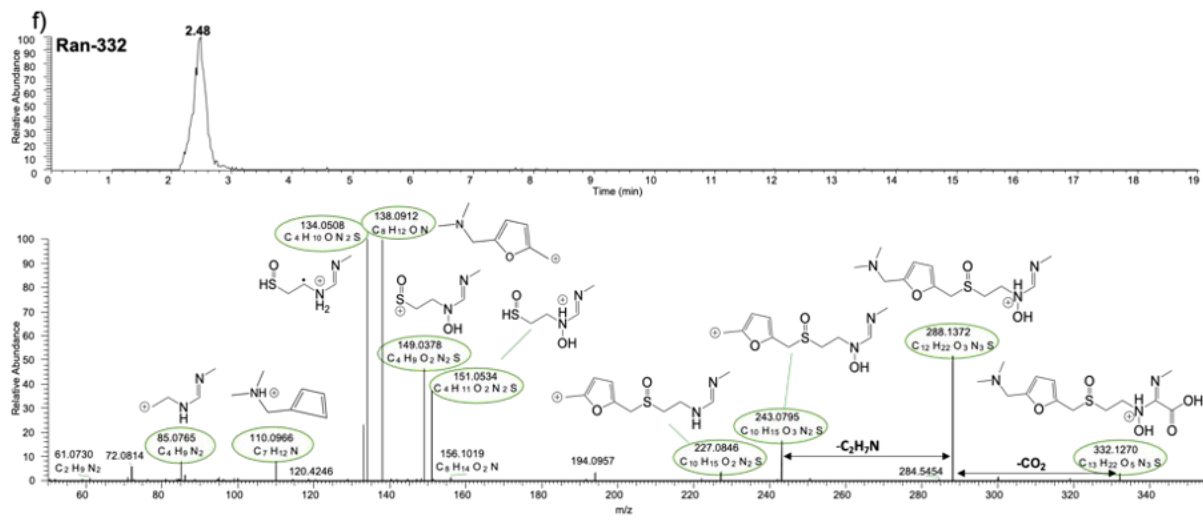
27

28

29

30
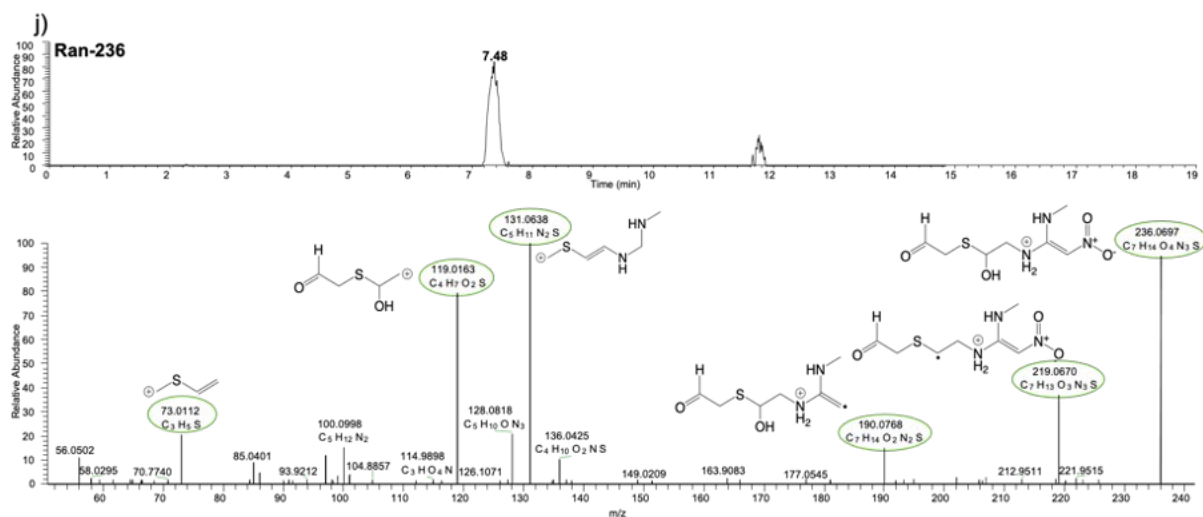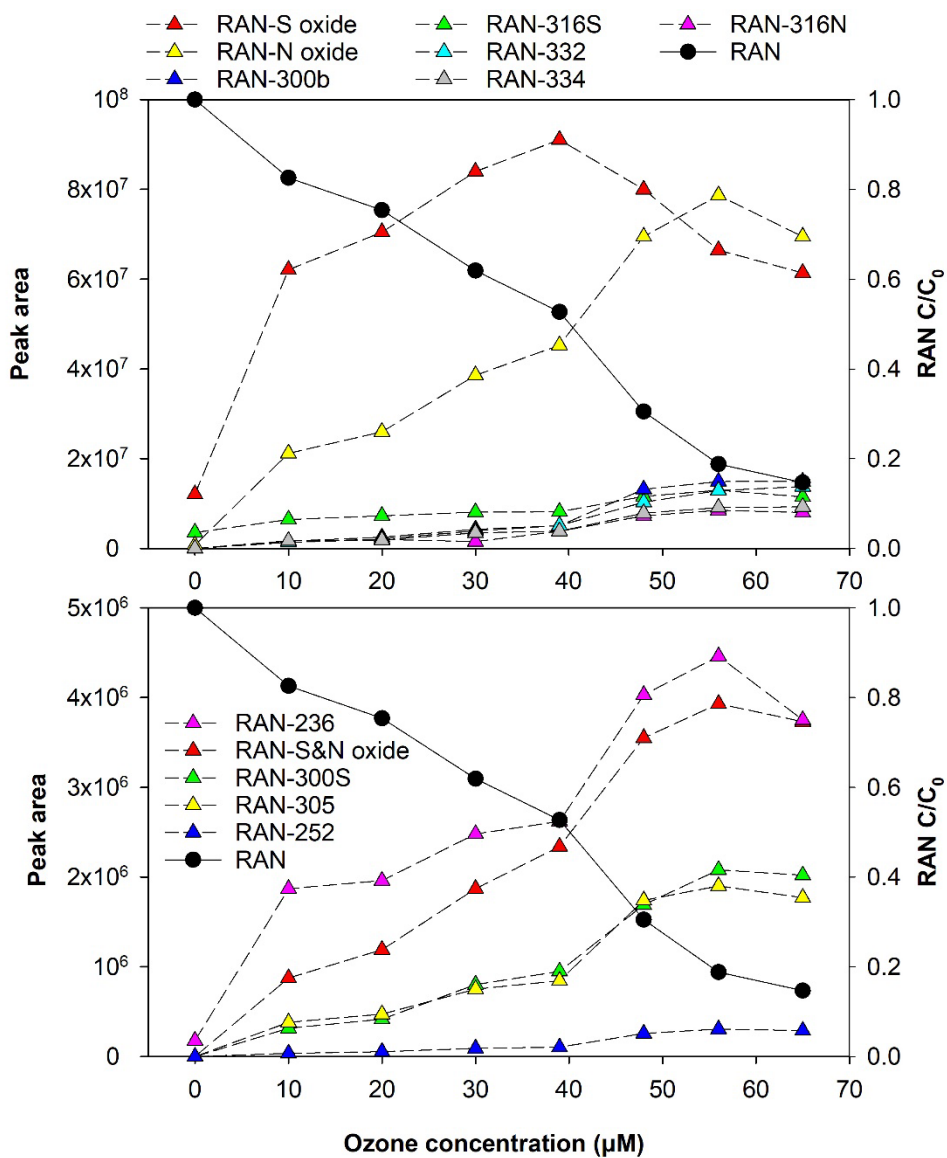
33

34
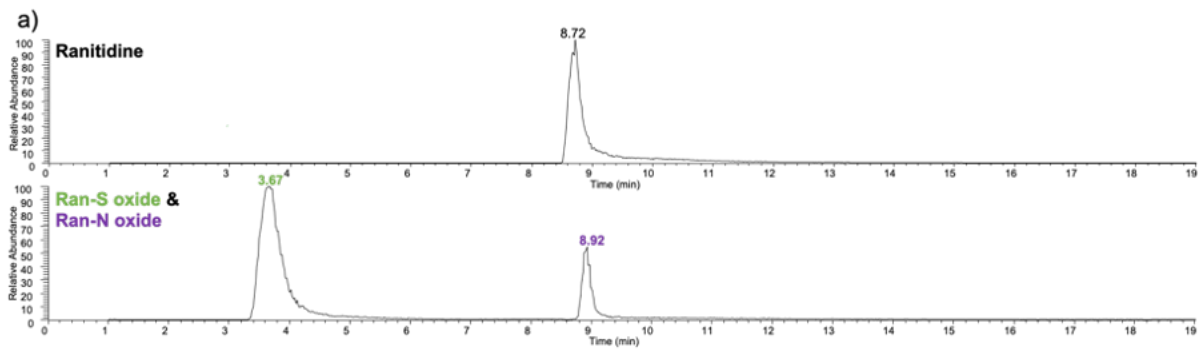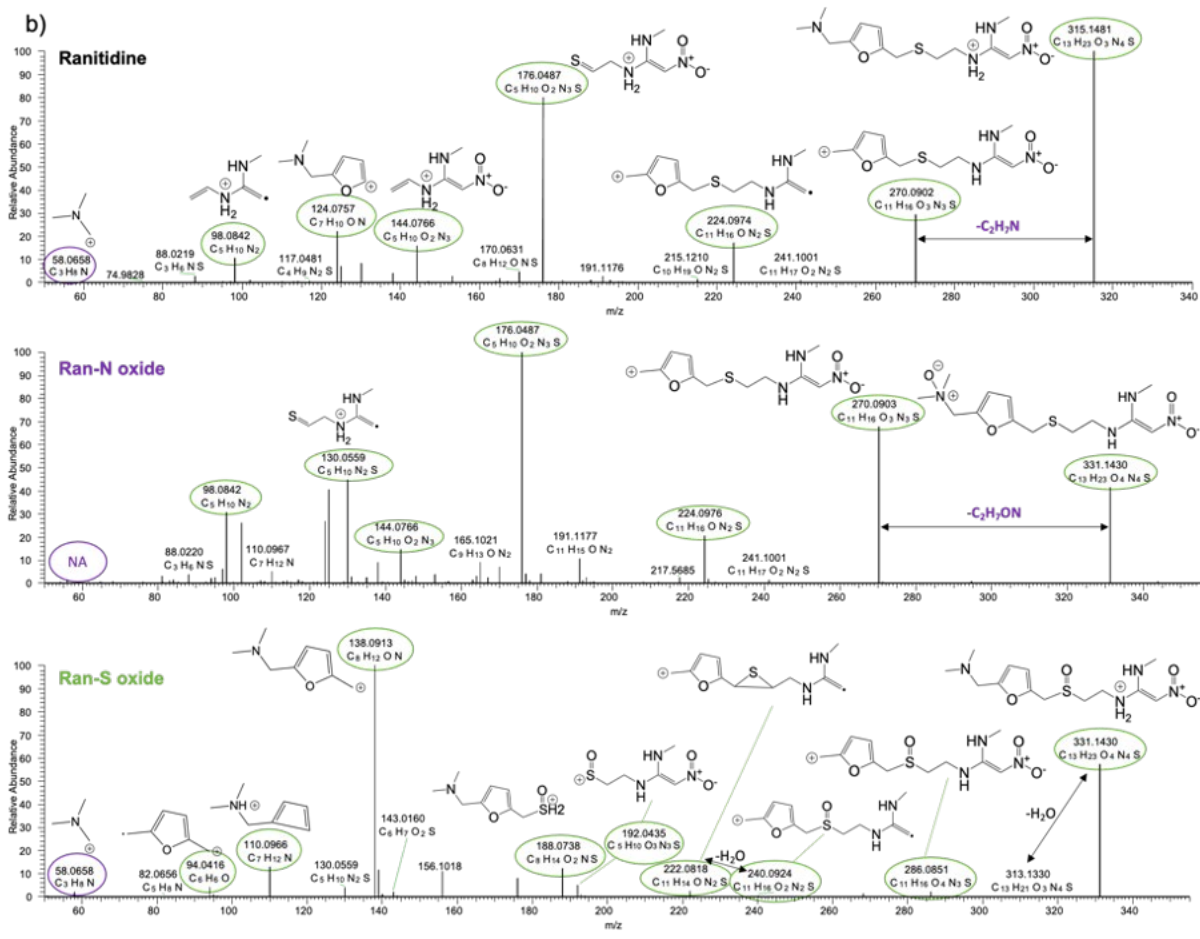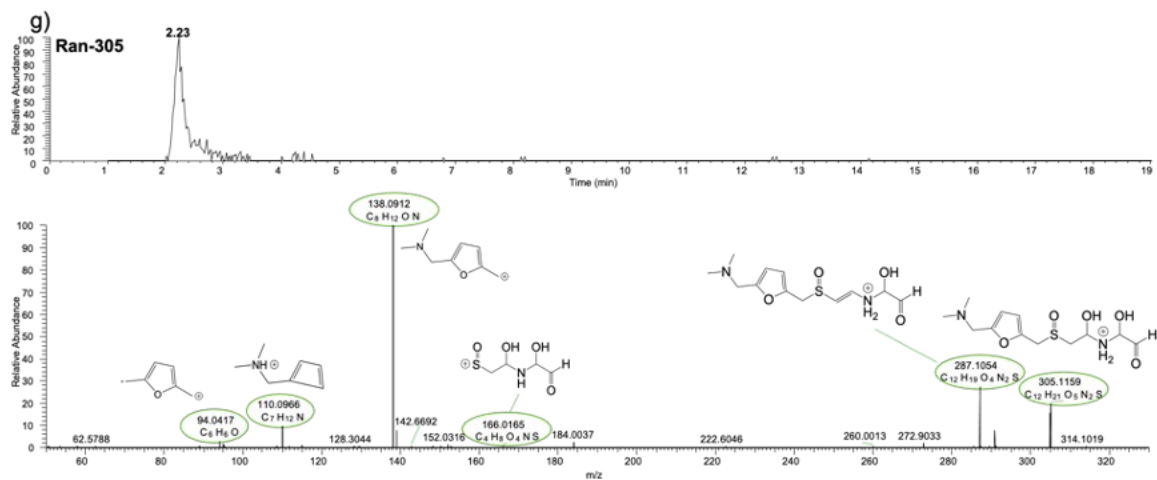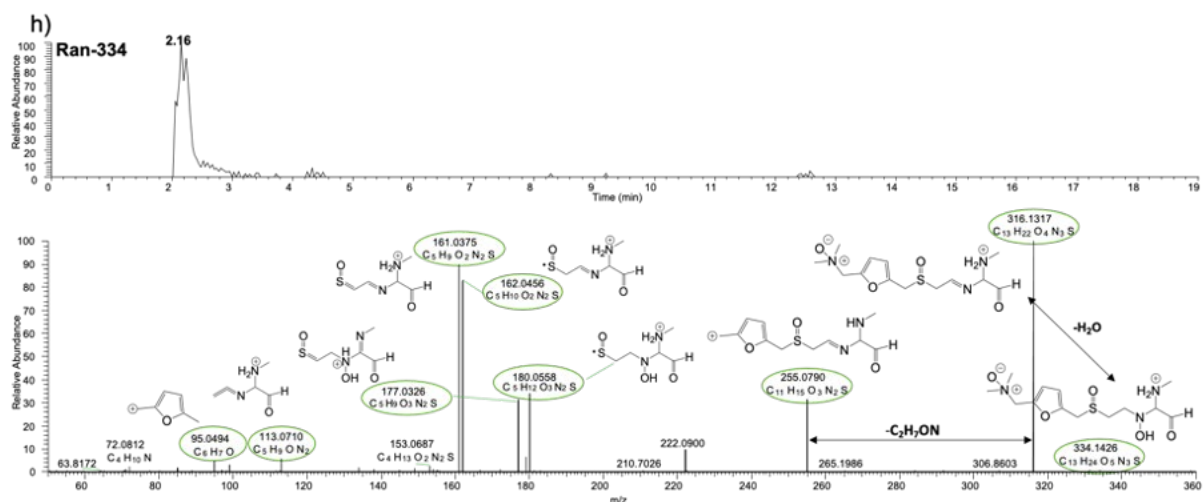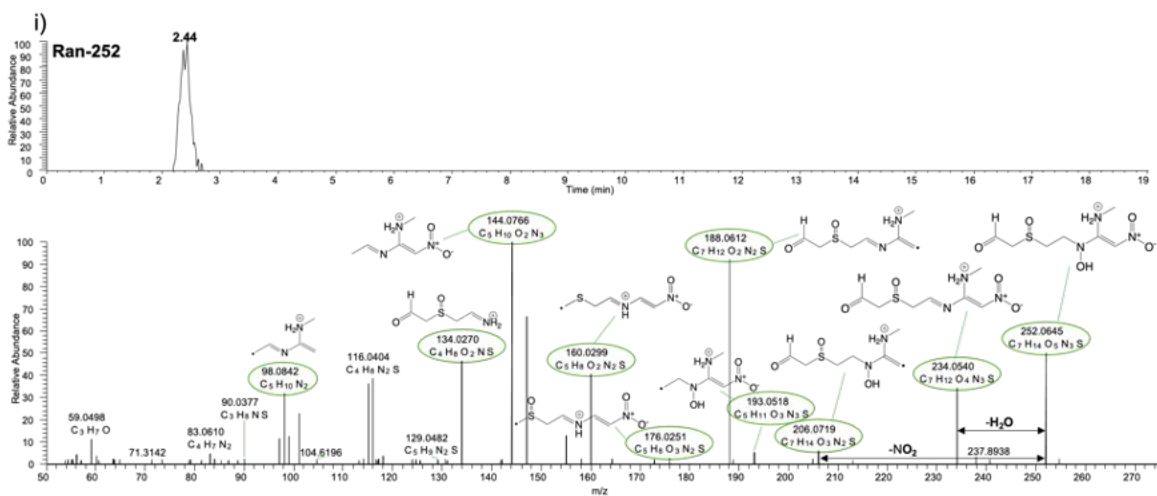
Figure S14. (a-j) Base peak chromatograms and MS^2 spectra including fragment structures for ranitidine and its transformation products identified in ozonation experiments (ranitidine initial concentration 50 μM).

Figure S15. Peak area of ranitidine (RAN) ozonation products and RAN degradation at different ozone concentrations. Data points are the average of duplicate experiments (error bars have been omitted). Ranitidine initial concentration 15 μM.
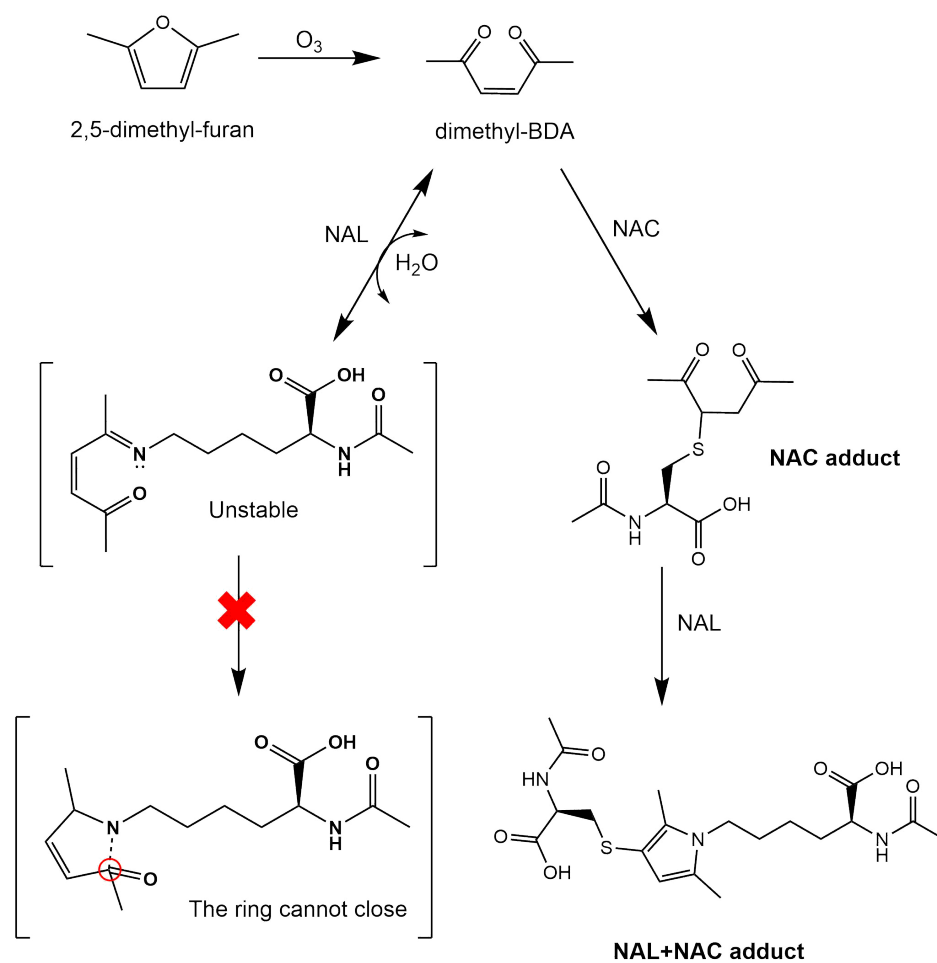
Figure S16. Reaction of dimethyl-BDA with NAL versus a NAL+NAC mixture, leading to formation of adducts detected with LC-HRMS.
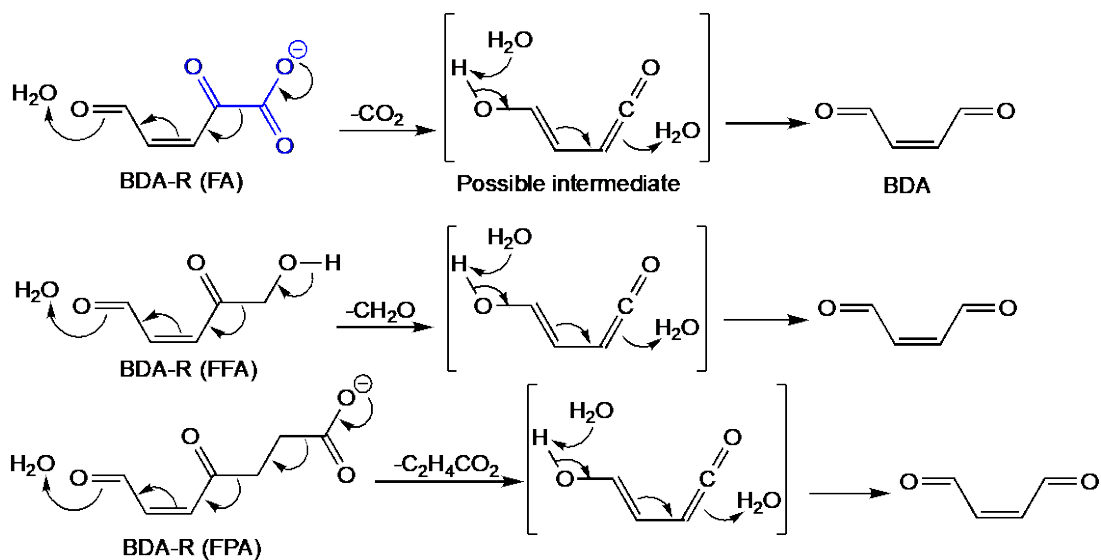
Figure S17. Suggested mechanisms for the cleavage of the substituent of BDA-R from FA, FFA and FPA in water, leading to the formation of BDA.

References

Aalizadeh, R., Nika, M.C. and Thomaidis, N.S. (2019) Development and application of retention time prediction models in the suspect and non-target screening of emerging contaminants. J Hazard Mater 363, 277-285.

Bader, H. and Hoigné, J. (1981) Determination of ozone in water by the indigo method. Water Research 15(4), 449-456.

Christophoridis, C., Nika, M.C., Aalizadeh, R. and Thomaidis, N.S. (2016) Ozonation of ranitidine: Effect of experimental parameters and identification of transformation products. Sci Total Environ 557-558, 170-182.

Huber, M.M., Canonica, S., Park, G.-Y. and von Gunten, U. (2003) Oxidation of Pharmaceuticals during Ozonation and Advanced Oxidation Processes. Environmental Science & Technology 37(5), 1016-1024.

Jeon, D., Kim, J., Shin, J., Hidayat, Z.R., Na, S. and Lee, Y. (2016) Transformation of ranitidine during water chlorination and ozonation: Moiety-specific reaction kinetics and elimination efficiency of NDMA formation potential. Journal of Hazardous Materials 318, 802-809.

Laurence, C., Rivard, M., Martens, T., Morin, C., Buisson, D., Bourcier, S., Sablier, M. and Oturan, M.A. (2014) Anticipating the fate and impact of organic environmental contaminants: a new approach applied to the pharmaceutical furosemide. Chemosphere 113, 193-199.